Imaging nuclear modifications on parton distributions at the LHC and EicC/EIC

Peng Ru / 茹芃

South China Normal University

In collaboration with
Meng-Quan Yang and Ben-Wei Zhang

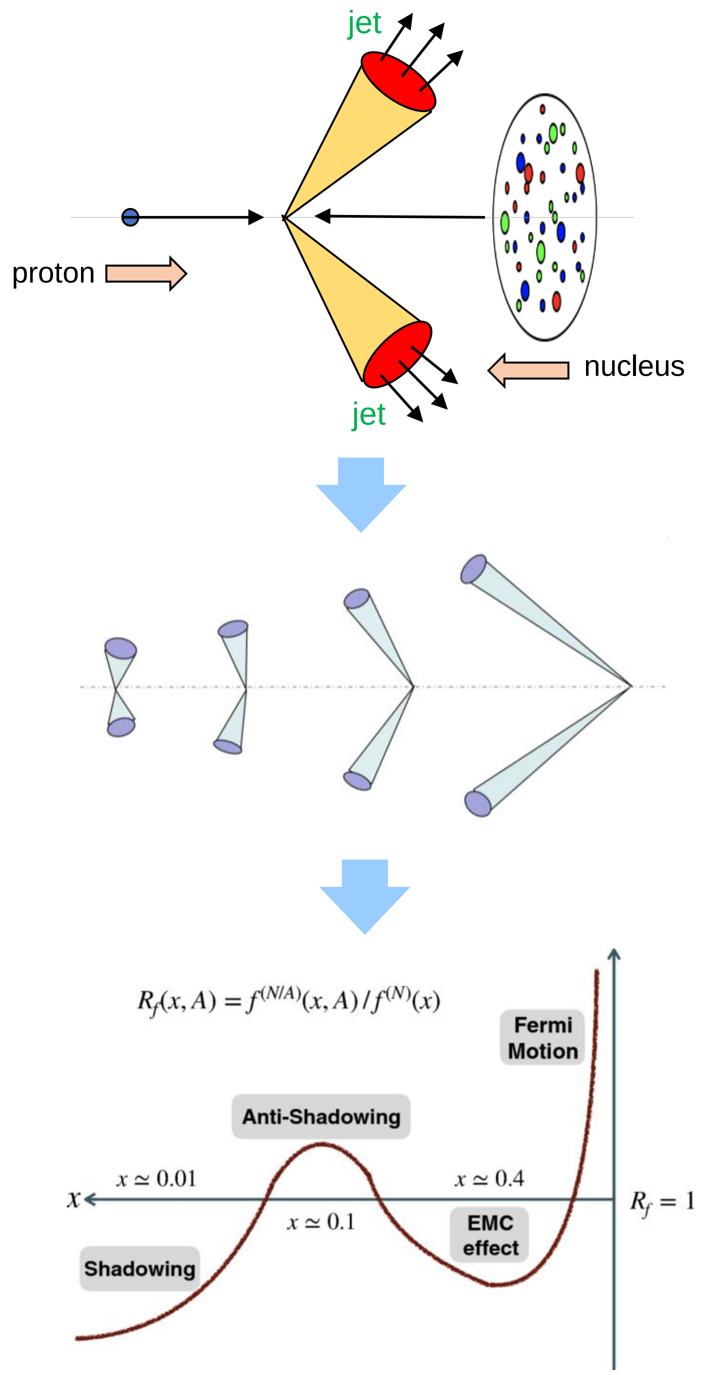

Part I: Background

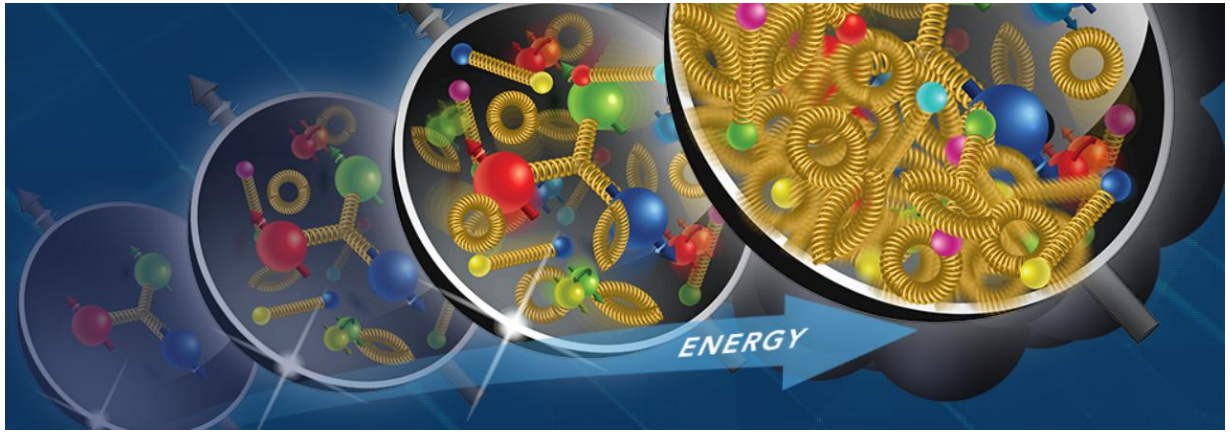

Partonic structures inside nucleon and nuclei:

-Fundamental to the study of QCD

-A key objective of upcoming experiments at EicC/EIC.

Part I: Background

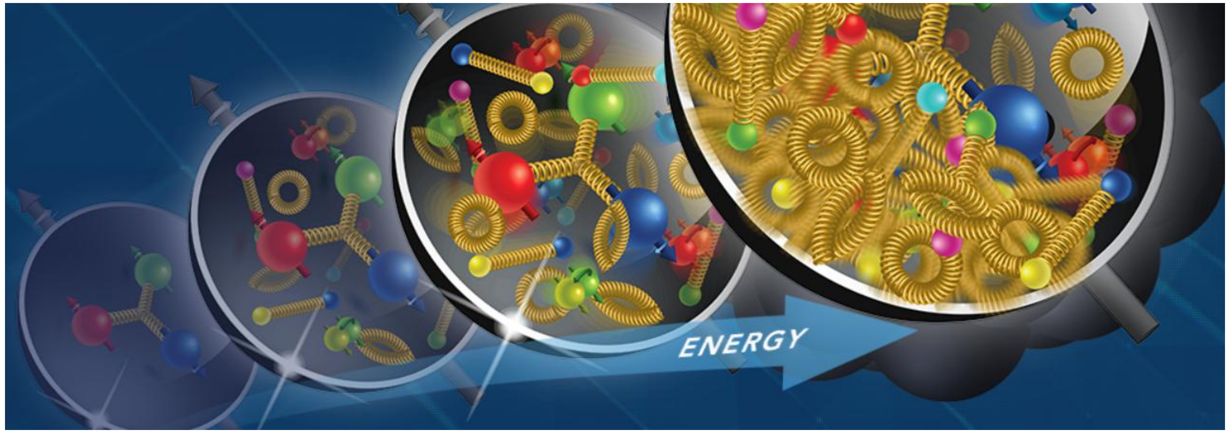

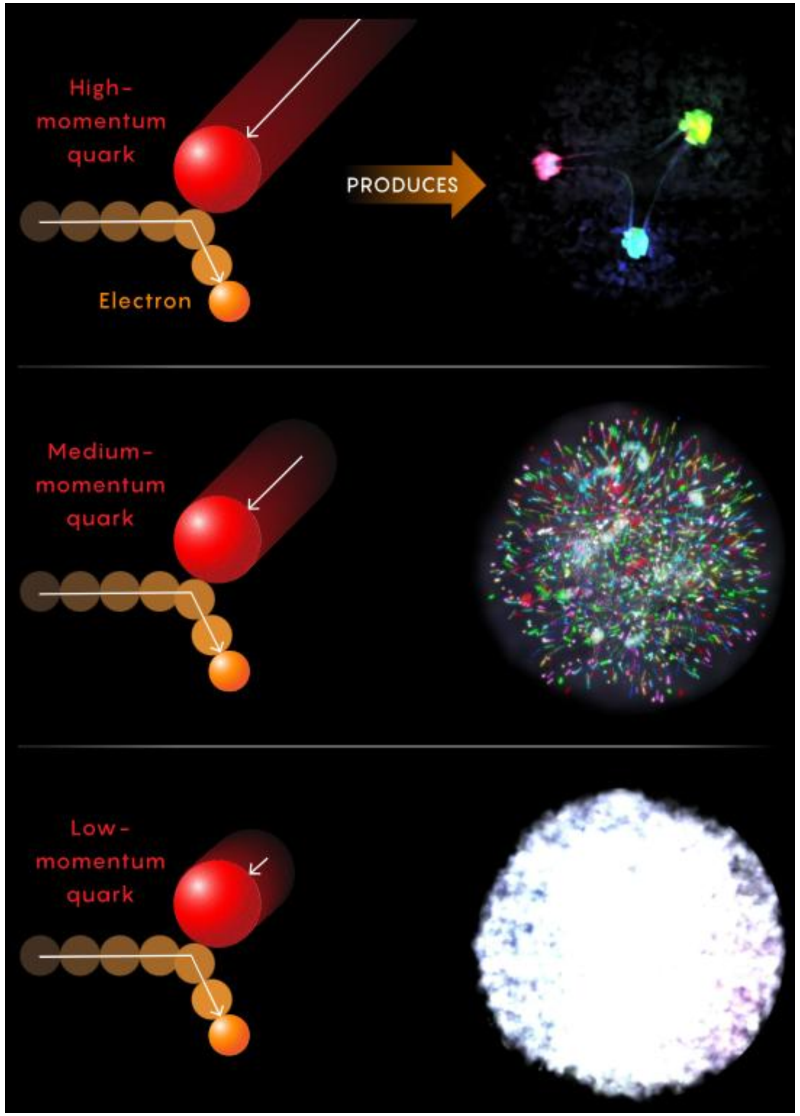

Partonic structures inside nucleon and nuclei:
-Fundamental to the study of QCD
-A key objective of upcoming experiments at EicC/EIC.

In high-energy collisions, partonic structure finds its concrete expression in the parton distribution functions (PDFs).

-Probability distribution of partons probed at certain energy scale.
-Indispensable non-perturbative inputs in the study of various hard scattering processes.

Part I: Background

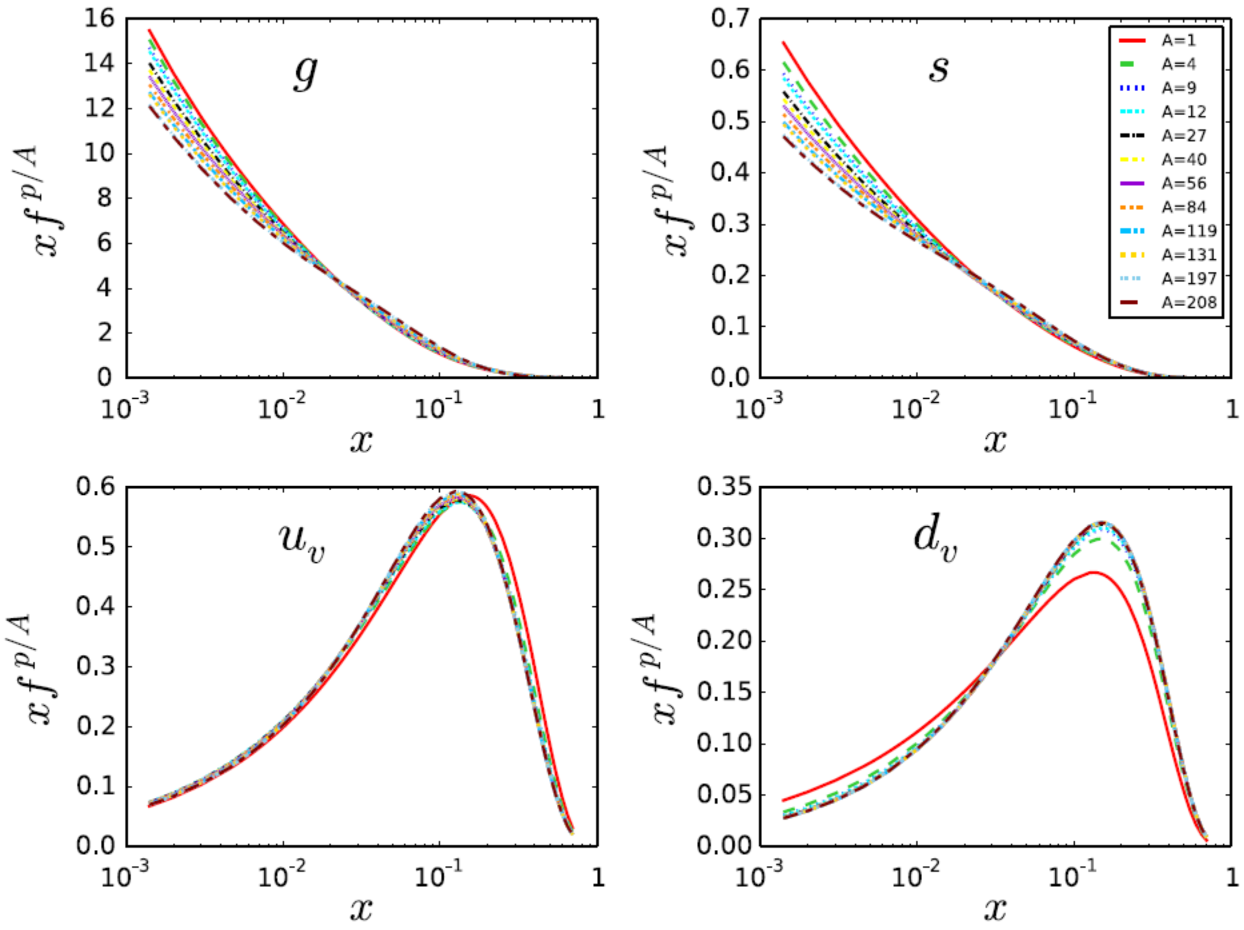

nCTEQ15, PRD 93, 085037 (2016)

Relative to the PDFs of free nucleon, environment of cold nuclear medium can affect the PDFs in nuclei.

Part I: Background

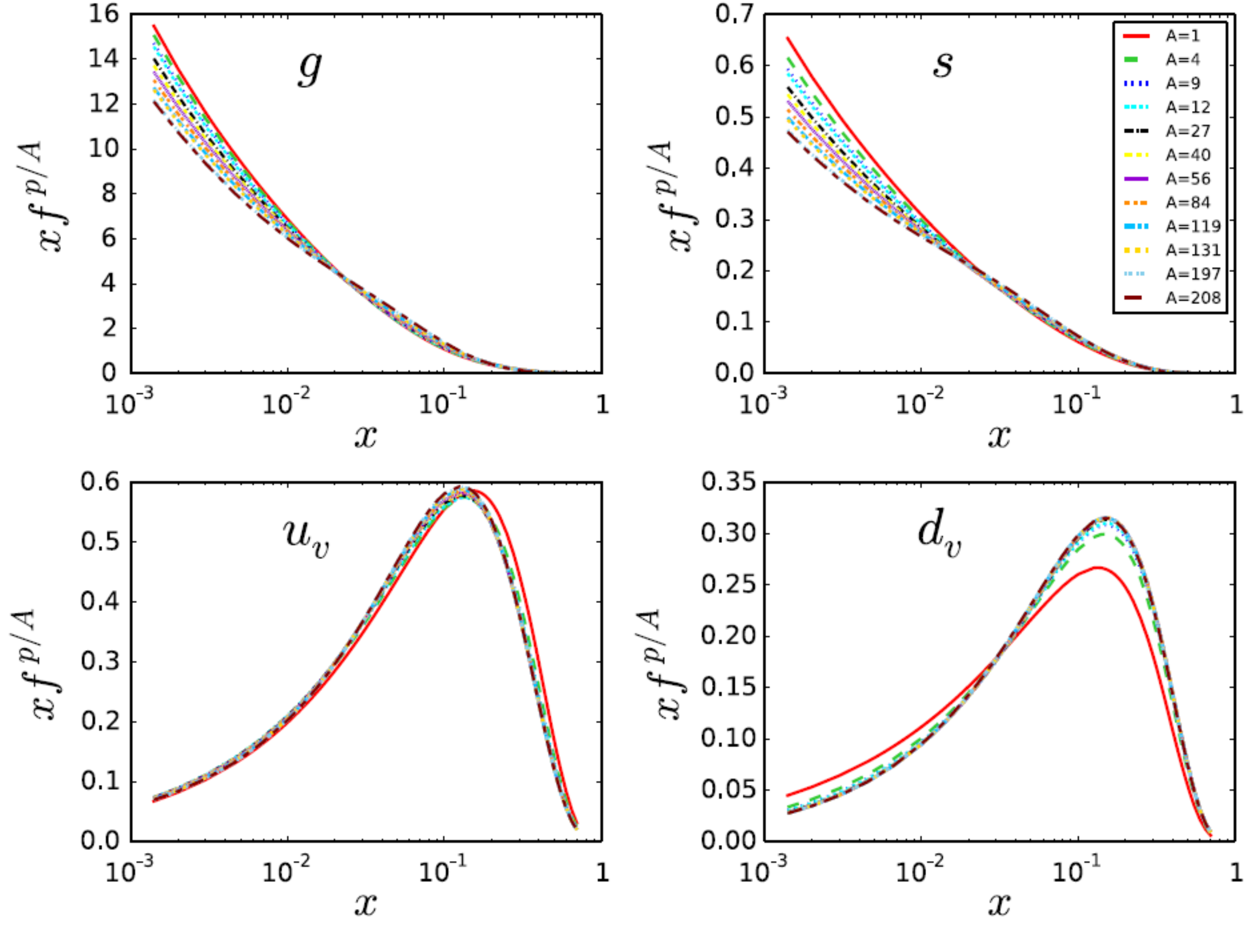

nCTEQ15, PRD 93, 085037 (2016)

$$r_i^A(x, Q^2) = \frac{f_i^{A,p}(x,Q^2)}{f_i^p(x,Q^2)}$$

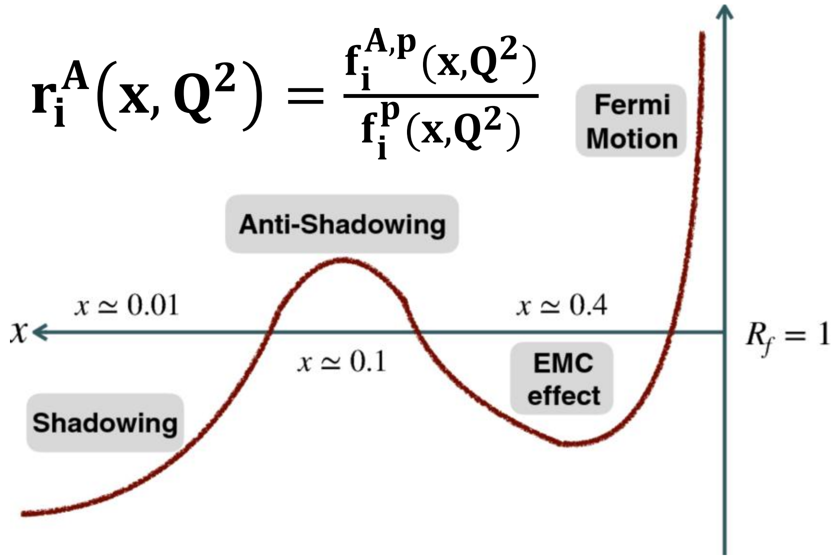

Nuclear modification ratios of collinear PDFs.

Relative to the PDFs of free nucleon, environment of cold nuclear medium can affect the PDFs in nuclei.

Part I: Background

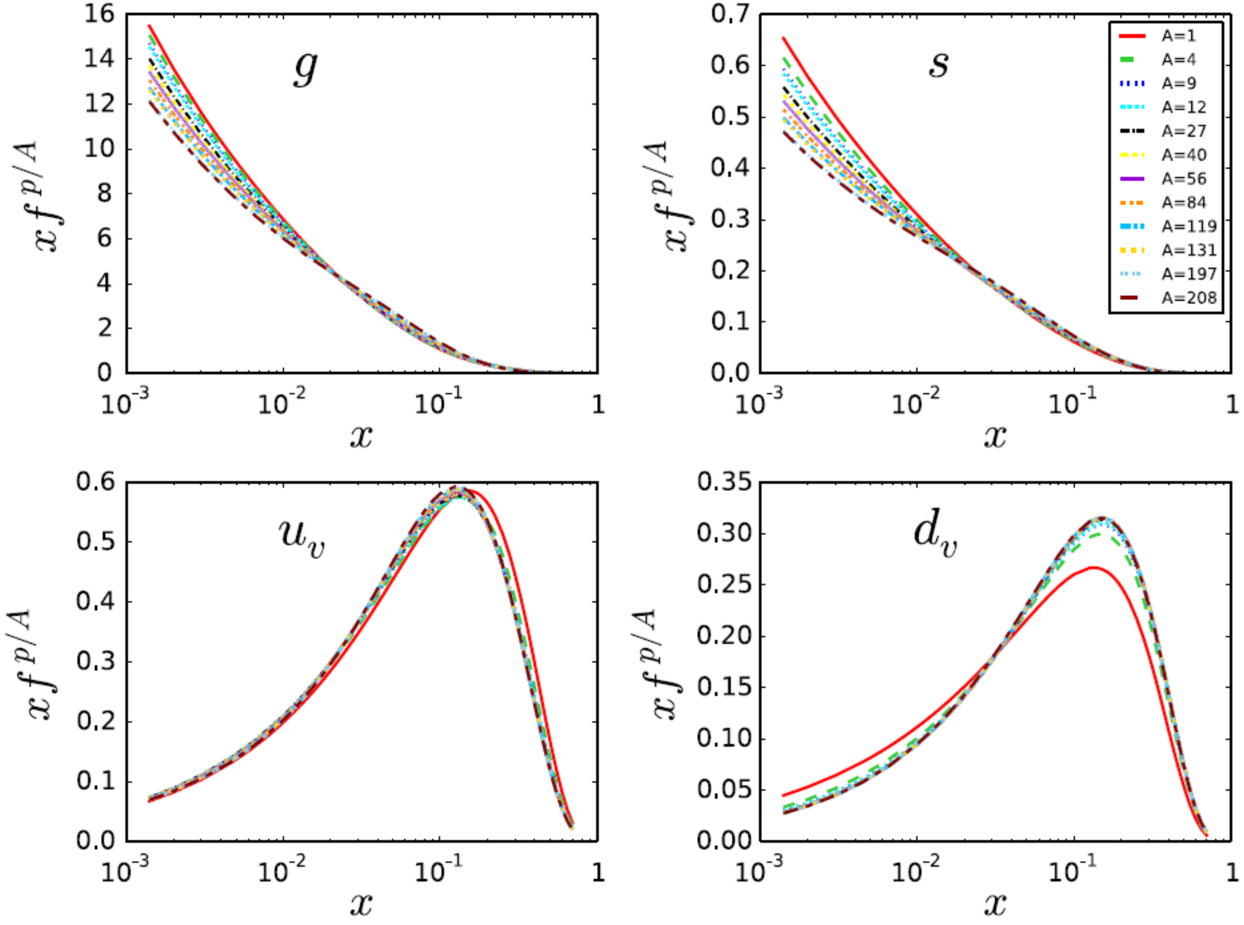

nCTEQ15, PRD 93, 085037 (2016)

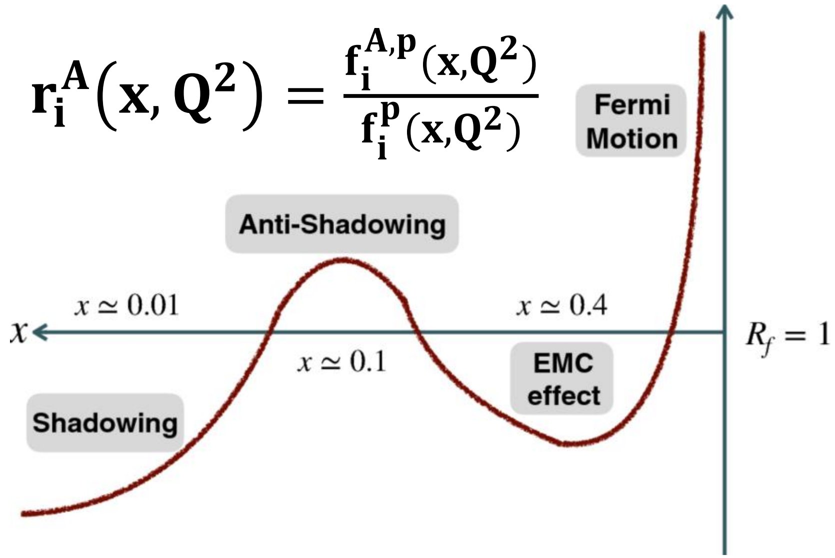

Nuclear modification ratios of collinear PDFs.

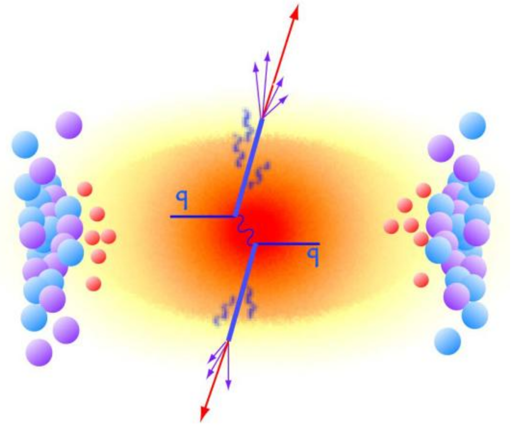

Relative to the PDFs of free nucleon, environment of cold nuclear medium can affect the PDFs in nuclei.

An essential baseline for disentangling final-state nuclear matter effects probed by hard particles.

Part I: Background

Eur. Phys. J. C (2017) 77:163

Table 1 The data sets used in the EPPS16 analysis, listed in the order of growing nuclear mass number. The number of data points and their contribution to χ^2 counts only those data points that fall within the kinematic cuts explained in the EPPS09 analysis are marked with

Experiment	Observable	Collisions	Data points
SLAC E139	DIS	e^-He(4), e^-D	21
CERN NMC 95, re	DIS	μ^-He(4), μ^-D	16
CERN NMC 95	DIS	μ^-Li(6), μ^-D	15
CERN NMC 95, Q^2 dep	DIS	μ^-Li(6), μ^-D	153
SLAC E139	DIS	e^-Be(9), e^-D	20
CERN NMC 96	DIS	μ^-Be(9), μ^-C	15
SLAC E139	DIS	e^-C(12), e^-D	7
CERN NMC 95	DIS	μ^-C(12), μ^-D	15
CERN NMC 95, Q^2 dep	DIS	μ^-C(12), μ^-D	165
CERN NMC 95, re	DIS	μ^-C(12), μ^-D	16
CERN NMC 95, re	DIS	μ^-C(12), μ^-Li(6)	20
FNAL E772	DY	pC(12), pD	9
SLAC E139	DIS	e^-Al(27), e^-D	20
CERN NMC 96	DIS	μ^-Al(27), μ^-C(12)	15
SLAC E139	DIS	e^-Ca(40), e^-D	7
FNAL E772	DY	pCa(40), pD	9
CERN NMC 95, re	DIS	μ^-Ca(40), μ^-D	15
CERN NMC 95, re	DIS	μ^-Ca(40), μ^-Li(6)	20
CERN NMC 9[illegible]	DIS	μ^-Ca(40), μ^-C(12)	15
SLAC E139	DIS	e^-Fe(56), e^-D	26
FNAL E772	DY	e^-Fe(56), e^-D	9
CERN NMC 96	DIS	μ^-Fe(56), μ^-C(12)	15
FNAL E866	DY	pFe(56), pBe(9)	28
CERN EMC	DIS	μ^-Cu(64), μ^-D	19
SLAC E139	DIS	e^-Ag(108), e^-D	7
CERN NMC 96	DIS	μ^-Sn(117), μ^-C(12)	15
CERN NMC 96, Q^2 dep	DIS	μ^-Sn(117), μ^-C(12)	144
FNAL E772	DY	pW(184), pD	9
FNAL E866	DY	pW(184), pBe(9)	28
CERN NA10[a]	DY	π^-W(184), π^-D	10
FNAL E615[a]	DY	π^+W(184), π^-W(184)	11
CERN NA3[a]	DY	π^-Pt(195), π^-H	7
SLAC E139	DIS	e^-Au(197), e^-D	21
RHIC PHENIX	π^0	dAu(197), pp	20
CERN NMC 96	DIS	μ^-Pb(207), μ^-C(12)	15
CERN CMS[a]	$W^\pm$	pPb(208)	10
CERN CMS[a]	Z	pPb(208)	6
CERN ATLAS[a]	Z	pPb(208)	7
CERN CMS[a]	dijet	pPb(208)	7
CERN CHORUS[a]	DIS	νPb(208), $\overline{\nu}$Pb(208)	824
Total			1811

Global QCD analysis

Both PDFs and their nuclear modification ratios rely on the global QCD analyses of diverse experimental data.

$$r_i^A(x, Q^2) = \frac{f_i^{A,p}(x,Q^2)}{f_i^{p}(x,Q^2)}$$

Part I: Background

Eur. Phys. J. C (2017) 77:163

Table 1 The data sets used in the EPPS16 analysis, listed in the order of growing nuclear mass number. The number of data points and their contribution to χ^2 counts only those data points that fall within the kinematic cuts explained in the EPPS09 analysis are marked with

Experiment	Observable	Collisions	Data points
SLAC E139	DIS	e^-He(4), e^-D	21
CERN NMC 95, re	DIS	μ^-He(4), μ^-D	16
CERN NMC 95	DIS	μ^-Li(6), μ^-D	15
CERN NMC 95, Q^2 dep	DIS	μ^-Li(6), μ^-D	153
SLAC E139	DIS	e^-Be(9), e^-D	20
CERN NMC 96	DIS	μ^-Be(9), μ^-C	15
SLAC E139	DIS	e^-C(12), e^-D	7
CERN NMC 95	DIS	μ^-C(12), μ^-D	15
CERN NMC 95, Q^2 dep	DIS	μ^-C(12), μ^-D	165
CERN NMC 95, re	DIS	μ^-C(12), μ^-D	16
CERN NMC 95, re	DIS	μ^-C(12), μ^-Li(6)	20
FNAL E772	DY	pC(12), pD	9
SLAC E139	DIS	e^-Al(27), [illegible]	20
CERN NMC 96	DIS	[illegible], μ^-C(12)	15
SLAC E139	DIS	e^-Ca(40), e^-D	7
FNAL E772	DY	pCa(40), pD	9
CERN NMC 95, re	DIS	μ^-Ca(40), μ^-D	15
CERN NMC 95, re	DIS	μ^-Ca(40), μ^-Li(6)	20
CERN N[illegible]	DIS	μ^-Ca(40), μ^-C(12)	15
SLAC E139	DIS	e^-Fe(56), e^-D	26
FNAL E772	DY	e^-Fe(56), e^-D	9
CERN NMC 96	DIS	μ^-Fe(56), μ^-C(12)	15
FNAL E866	DY	pFe(56), pBe(9)	28
CERN EMC	DIS	μ^-Cu(64), μ^-D	19
SLAC E139	DIS	e^-Ag(108), e^-D	7
CERN NMC 96	DIS	μ^-Sn(117), μ^-C(12)	15
CERN NMC 96, Q^2 dep	DIS	μ^-Sn(117), μ^-C(12)	144
FNAL E772	DY	pW(184), pD	9
FNAL E866	DY	pW(184), pBe(9)	28
CERN NA10[a]	DY	π^-W(184), π^-D	10
FNAL E615[a]	DY	π^+W(184), π^-W(184)	11
CERN NA3[a]	DY	π^-Pt(195), π^-H	7
SLAC E139	DIS	e^-Au(197), e^-D	21
RHIC PHENIX	π^0	dAu(197), pp	20
CERN NMC 96	DIS	μ^-Pb(207), μ^-C(12)	15
CERN CMS[a]	$W^\pm$	pPb(208)	10
CERN CMS[a]	Z	pPb(208)	6
CERN ATLAS[a]	Z	pPb(208)	7
CERN CMS[a]	dijet	pPb(208)	7
CERN CHORUS[a]	DIS	νPb(208), $\bar{\nu}$Pb(208)	824
Total			1811

Global QCD analysis

Both PDFs and their nuclear modification ratios rely on the global QCD analyses of diverse experimental data.

$$\mathbf{r_i^A(x, Q^2) = \frac{f_i^{A,p}(x,Q^2)}{f_i^{p}(x,Q^2)}}$$

Challenge in global analyses:

In the theoretical prediction for a realistic observable, the dependencies on x, Q2, and i are intricately convoluted in calculations with collinear factorization in perturbative QCD.

$$d\sigma = \sum_{a,b,c}\int dx_a \int dx_b \int dz_c \boxed{f_a(x_a,\mu)}\boxed{f_b(x_b,\mu)}\boxed{D_c^h(z_c,\mu)}\boxed{d\hat{\sigma}_{ab}^c(x_aP_A, x_bP_B, P_h/z_c, \mu)}$$

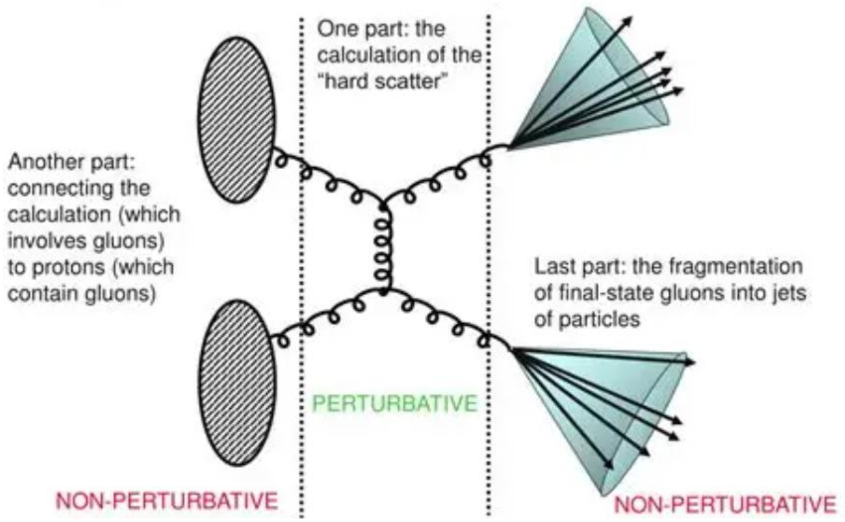

Challenge in global analyses:
An analogy to solving a system of equations

$$\begin{cases} a_{11}x_1 + a_{12}x_2 + \cdots + a_{1n}x_n = O_1 \\ a_{21}x_1 + a_{22}x_2 + \cdots + a_{2n}x_n = O_2 \\ \vdots \\ \vdots \\ a_{n1}x_1 + a_{n2}x_2 + \cdots + a_{nn}x_n = O_n \end{cases}$$

⬇

$$\{x_1, x_2, \cdots, x_n\}$$

Part I: Background

Challenge in global analyses:
An analogy to solving a system of equations

$$\begin{cases} a_{11}x_1 + a_{12}x_2 + \cdots + a_{1n}x_n = O_1 \\ a_{21}x_1 + a_{22}x_2 + \cdots + a_{2n}x_n = O_2 \\ \vdots \\ \vdots \\ a_{n1}x_1 + a_{n2}x_2 + \cdots + a_{nn}x_n = O_n \end{cases}$$

$$\{x_1, x_2, \cdots, x_n\}$$

Lower degree of variable mixing results in faster solving.

$$\begin{cases} a_{11}x_1 = O_1 \\ a_{21}x_1 + a_{22}x_2 = O_2 \\ \vdots \\ \vdots \\ a_{nn}x_n = O_n \end{cases}$$

$$\{x_1, x_2, \cdots, x_n\}$$

Part I: Background

Challenge in global analyses:
An analogy to solving a system of equations

$$r_i^A(x, Q^2) = \frac{f_i^{A,p}(x,Q^2)}{f_i^p(x,Q^2)}$$

$$\begin{cases} a_{11}x_1 + a_{12}x_2 + \cdots + a_{1n}x_n = O_1 \\ a_{21}x_1 + a_{22}x_2 + \cdots + a_{2n}x_n = O_2 \\ \vdots \\ a_{n1}x_1 + a_{n2}x_2 + \cdots + a_{nn}x_n = O_n \end{cases}$$

Experimental uncertainties

Theoretical uncertainties

$$\{x_1, x_2, \cdots, x_n\}$$

$$\begin{cases} a_{11}x_1 = O_1 \\ a_{21}x_1 + a_{22}x_2 = O_2 \\ \vdots \\ a_{nn}x_n = O_n \end{cases}$$

$$\{x_1, x_2, \cdots, x_n\}$$

Challenge in global analyses:
An analogy to solving a system of equations

$$r_i^A(x, Q^2) = \frac{f_i^{A,p}(x,Q^2)}{f_i^p(x,Q^2)}$$

$$\begin{cases} a_{11}x_1 + a_{12}x_2 + \cdots + a_{1n}x_n = O_1 \\ a_{21}x_1 + a_{22}x_2 + \cdots + a_{2n}x_n = O_2 \\ \vdots \\ a_{n1}x_1 + a_{n2}x_2 + \cdots + a_{nn}x_n = O_n \end{cases}$$

Experimental uncertainties

Theoretical uncertainties

$$\{x_1, x_2, \cdots, x_n\}$$

$$\begin{cases} a_{11}x_1 = O_1 \\ a_{21}x_1 + a_{22}x_2 = O_2 \\ \vdots \\ a_{nn}x_n = O_n \end{cases}$$

$$\{x_1, x_2, \cdots, x_n\}$$

Challenge in global analyses:
An analogy to solving a system of equations

$$r_i^A(x, Q^2) = \frac{f_i^{A,p}(x,Q^2)}{f_i^p(x,Q^2)}$$

$$\begin{cases} a_{11}x_1 + a_{12}x_2 + \cdots + a_{1n}x_n = O_1 \\ a_{21}x_1 + a_{22}x_2 + \cdots + a_{2n}x_n = O_2 \\ \vdots \\ a_{n1}x_1 + a_{n2}x_2 + \cdots + a_{nn}x_n = O_n \end{cases}$$

Experimental uncertainties

Theoretical uncertainties

$$\{x_1, x_2, \cdots, x_n\}$$

$$\begin{cases} a_{11}x_1 = O_1 \\ a_{21}x_1 + a_{22}x_2 = O_2 \\ \vdots \\ a_{nn}x_n = O_n \end{cases}$$

$$\{x_1, x_2, \cdots, x_n\}$$

Challenge from mixing contributions of variables
1. Overfitting.
2. Parameters degeneracy.
3. Complicated uncertainty propagation.
4. Slow and unstable convergence.

Part I: Background

Challenge in global analyses:
An analogy to solving a system of equations

$$r_i^A(x, Q^2) = \frac{f_i^{A,p}(x,Q^2)}{f_i^p(x,Q^2)}$$

$$\begin{cases} a_{11}x_1 + a_{12}x_2 + \cdots + a_{1n}x_n = O_1 \\ a_{21}x_1 + a_{22}x_2 + \cdots + a_{2n}x_n = O_2 \\ \vdots \\ a_{n1}x_1 + a_{n2}x_2 + \cdots + a_{nn}x_n = O_n \end{cases}$$

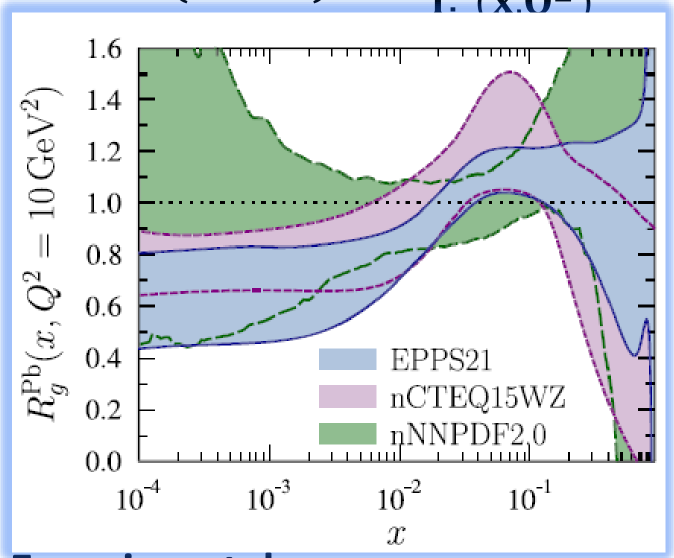

Experimental uncertainties

$$\begin{cases} a_{11}x_1 = O_1 \\ a_{21}x_1 + a_{22}x_2 = O_2 \\ \vdots \\ a_{nn}x_n = O_n \end{cases}$$

Theoretical uncertainties

$$\{x_1, x_2, \cdots, x_n\}$$

Challenge from mixing contributions of variables
1. Overfitting.
2. Parameters degeneracy.
3. Complicated uncertainty propagation.
4. Slow and unstable convergence.

$$\{x_1, x_2, \cdots, x_n\}$$

Insights from nuclear binding dynamics are useful.

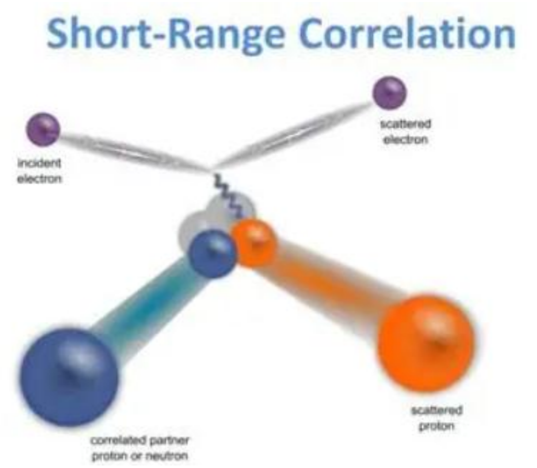

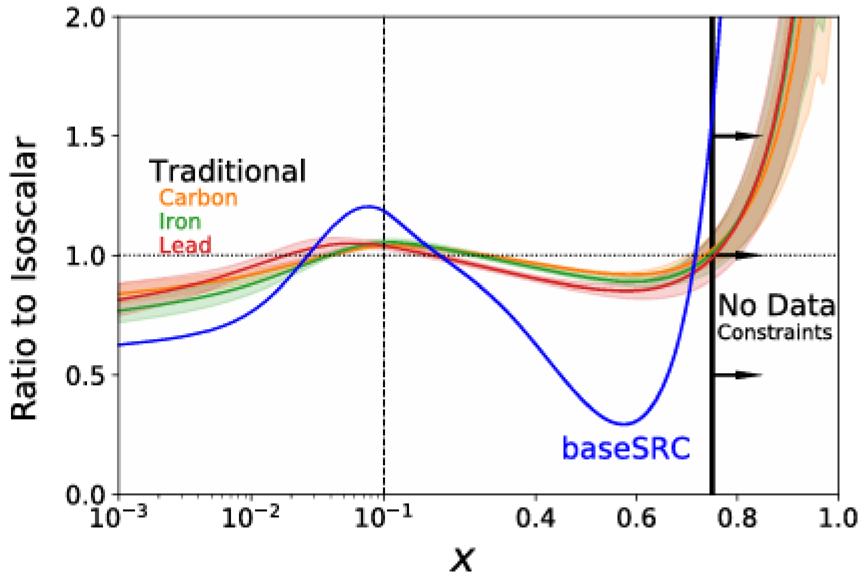

nCTEQ, PRL 133, 152502 (2024)

Part I: Background

Insights from nuclear binding dynamics are useful.

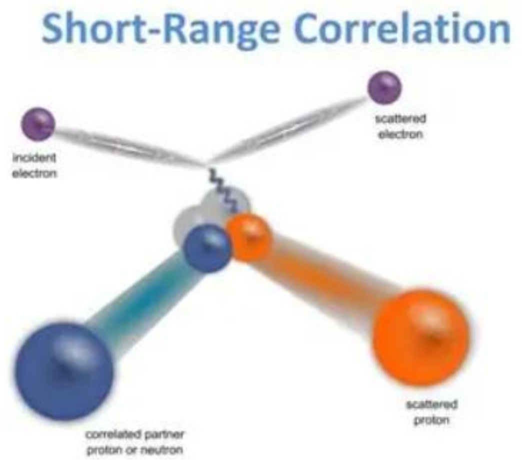

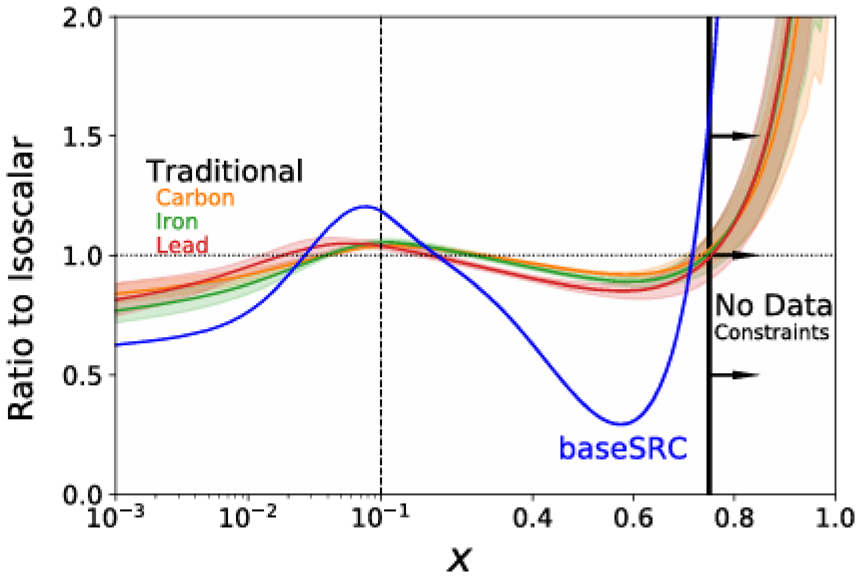

nCTEQ, PRL 133, 152502 (2024)

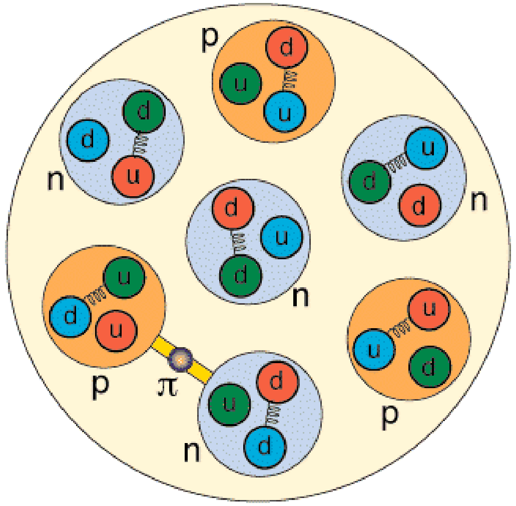

Meson exchange current
Off-shell corrections
Coherent nuclear shadowing
Fermi motion
……

Kulagin and Petti, PRC 90, 045204 (2014).

Part I: Background

Data of nuclear modifications to structure function in DIS serve as an effective image of $r_i^A(x, Q^2)$

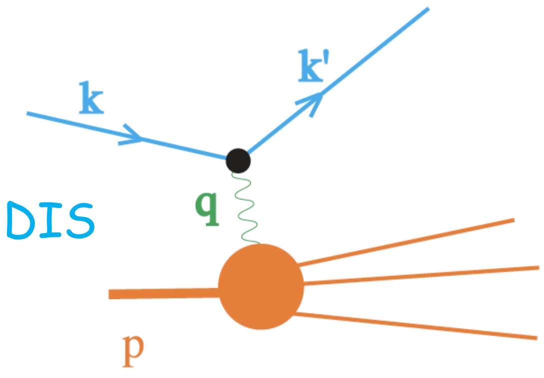

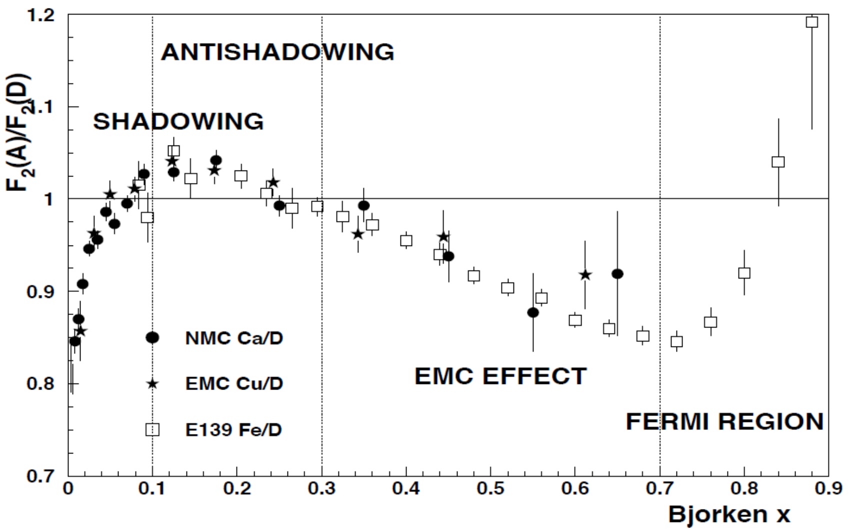

Part I: Background

Data of nuclear modifications to structure function in DIS serve as an effective image of $r_i^A(x, Q^2)$

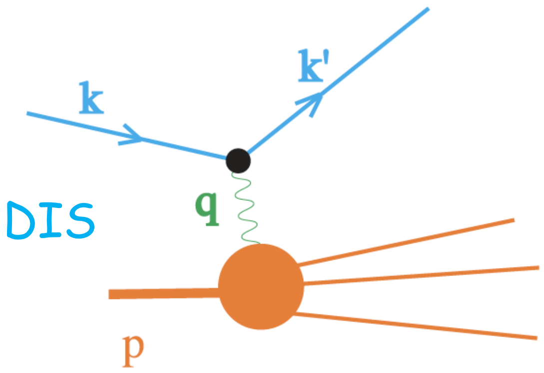

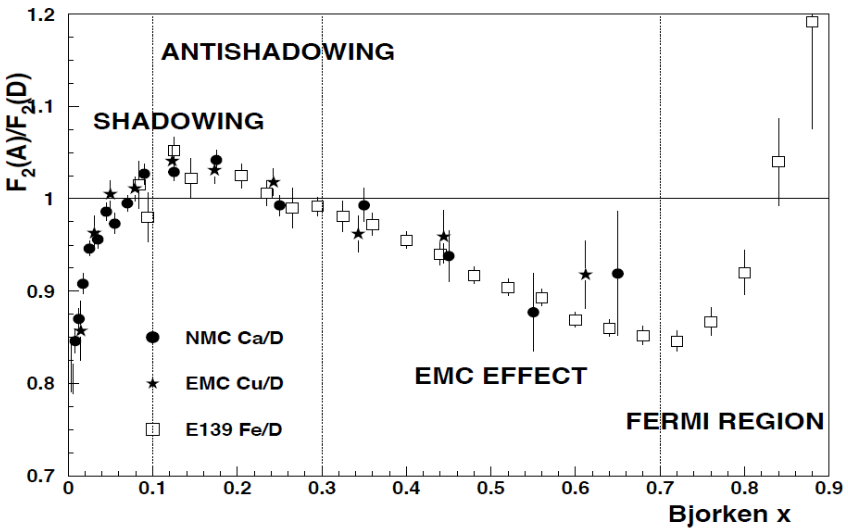

$$r_i^A(x, Q^2) = \frac{f_i^{A,p}(x,Q^2)}{f_i^p(x,Q^2)}$$

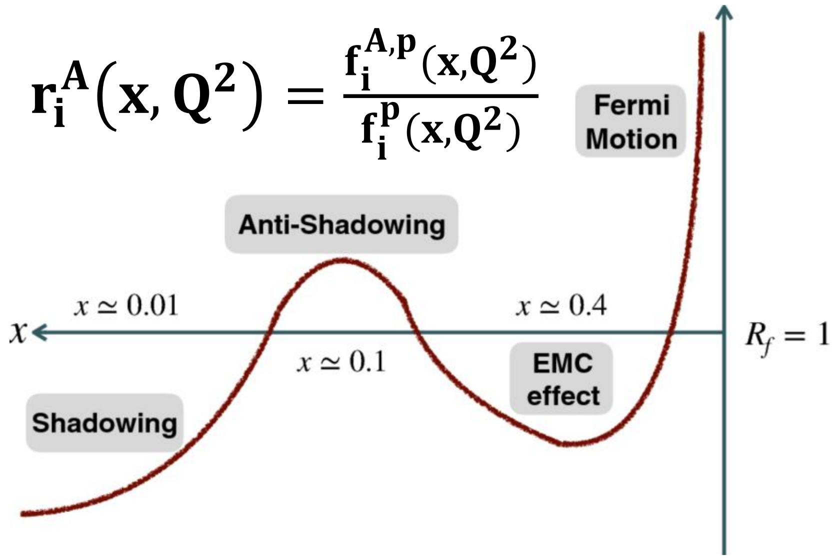

Measurement of such observable with low degree of variable mixing:

1. inspire parametrizations of modifications

2. improve the efficiency of global analysis.

Status for pA collisions at the LHC

The vast amount of data from the Large Hadron Collider (LHC) has revolutionized global analyses over the past decade.

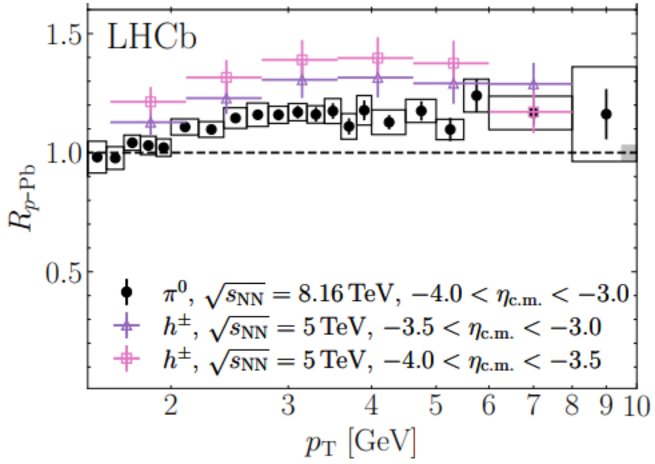

LHCb Collaboration
PRL (2023)

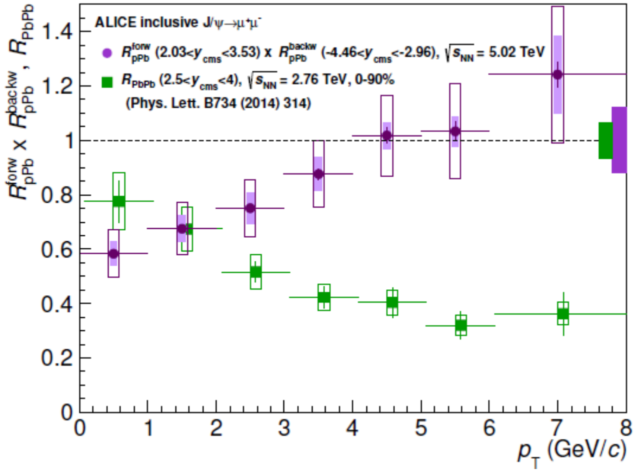

ALICE Collaboration
JHEP 06(2015) 055

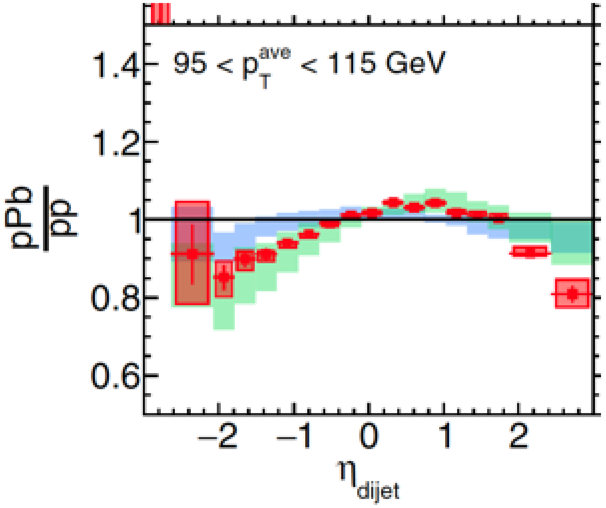

CMS, PRL 121, 062002 (2018)

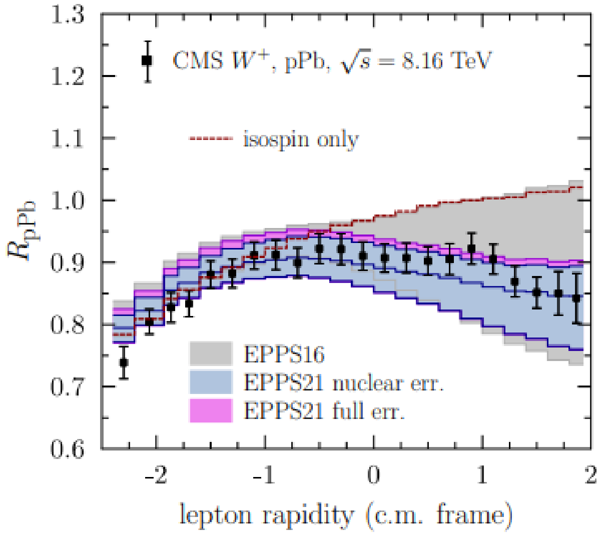

CMS, PLB (2020)

Part I: Background

Status for pA collisions at the LHC

The vast amount of data from the Large Hadron Collider (LHC) has revolutionized global analyses over the past decade.

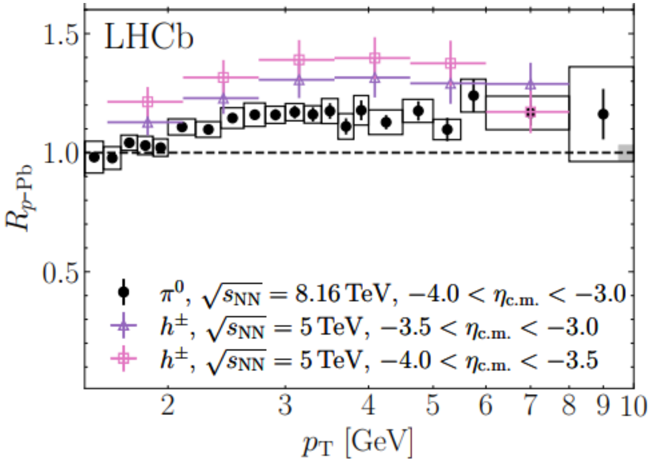

LHCb Collaboration
PRL (2023)

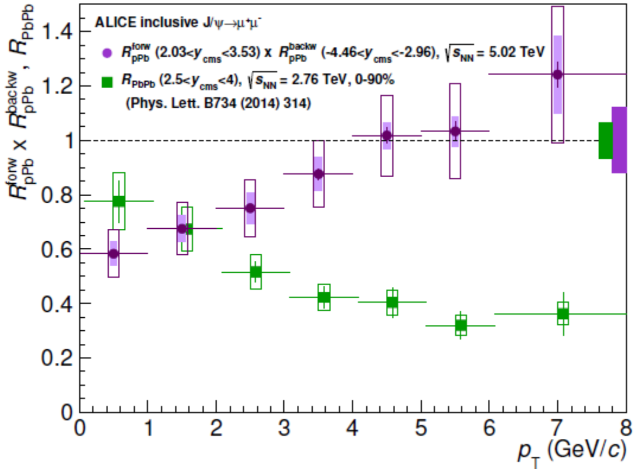

ALICE Collaboration
JHEP 06(2015) 055

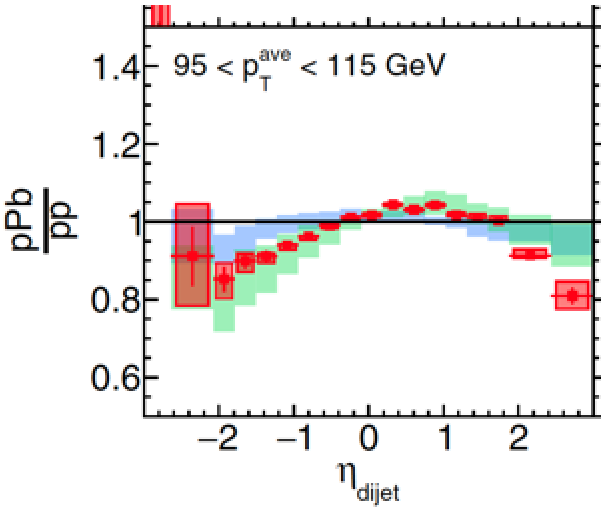

CMS, PRL 121, 062002 (2018)

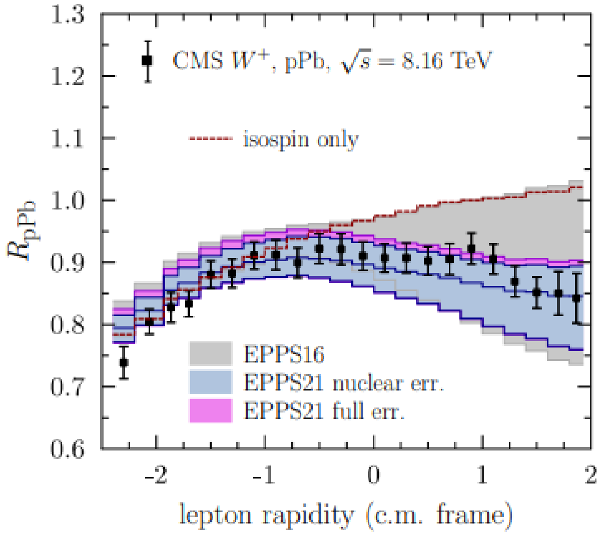

CMS, PLB (2020)

However, traditional measurements exhibit a less direct mapping to PDFs.
The imaging of $r_i^A(x, Q^2)$ achieved in DIS has not been replicated for most LHC processes.

Can we image $r_i^A(x, Q^2)$ at the LHC?

Part 2: Construction of the image of $r_i^A(x, Q^2)$ in pA

Analyses based on traditional observables

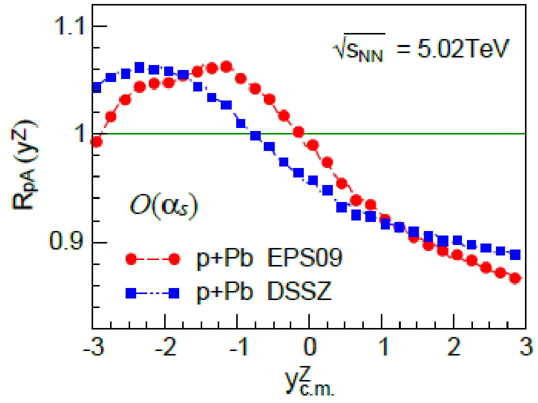

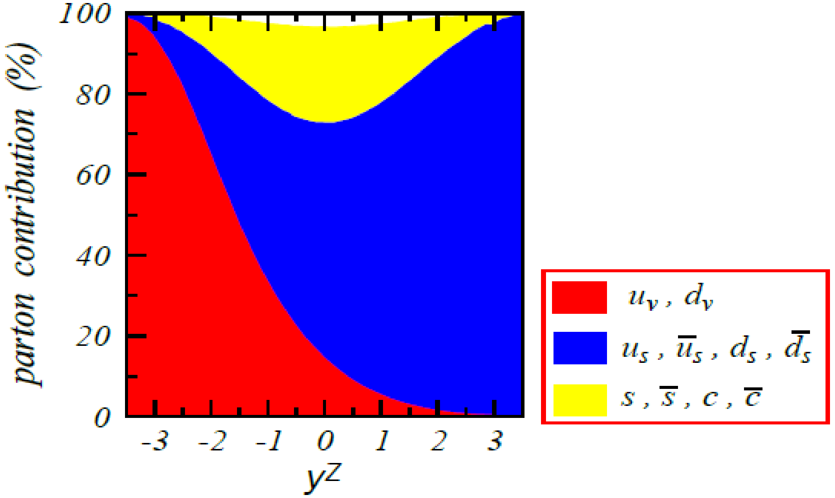

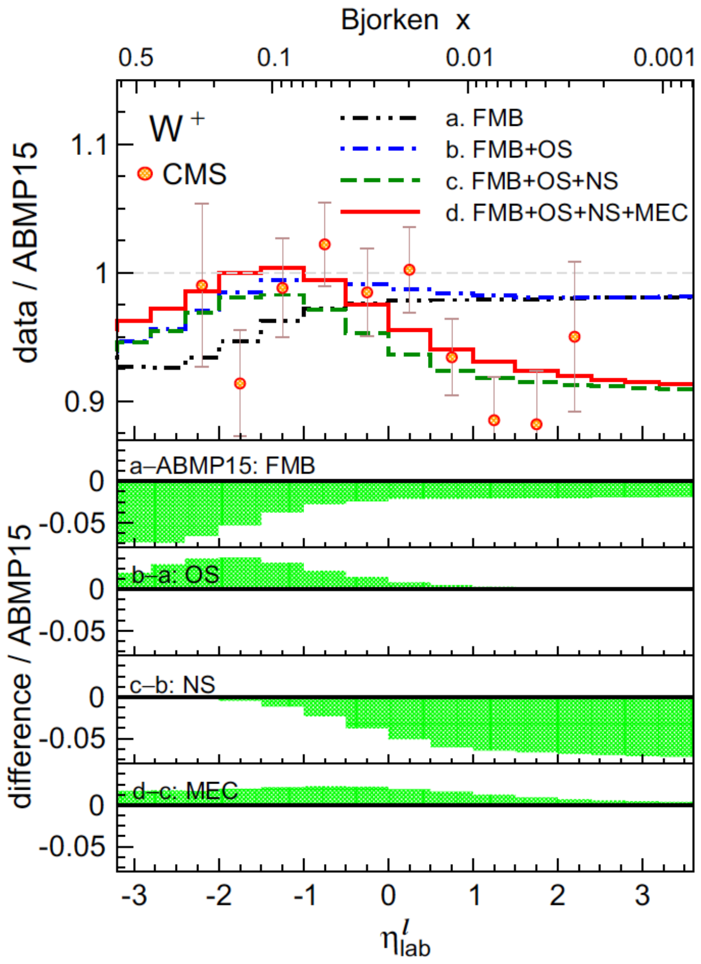

Understanding of R_{pA} at partonic level

Understanding of R_{pA} with binding dynamics

Ru, Wang, Zhang, Zhang, EPJC 75,426 (2015)

Ru, Kulagin, Petti, Zhang, PRD 94, 113013 (2016)

Part 2: Construction of the image of $r_i^A(x, Q^2)$ in pA

Triply differential dijet cross section

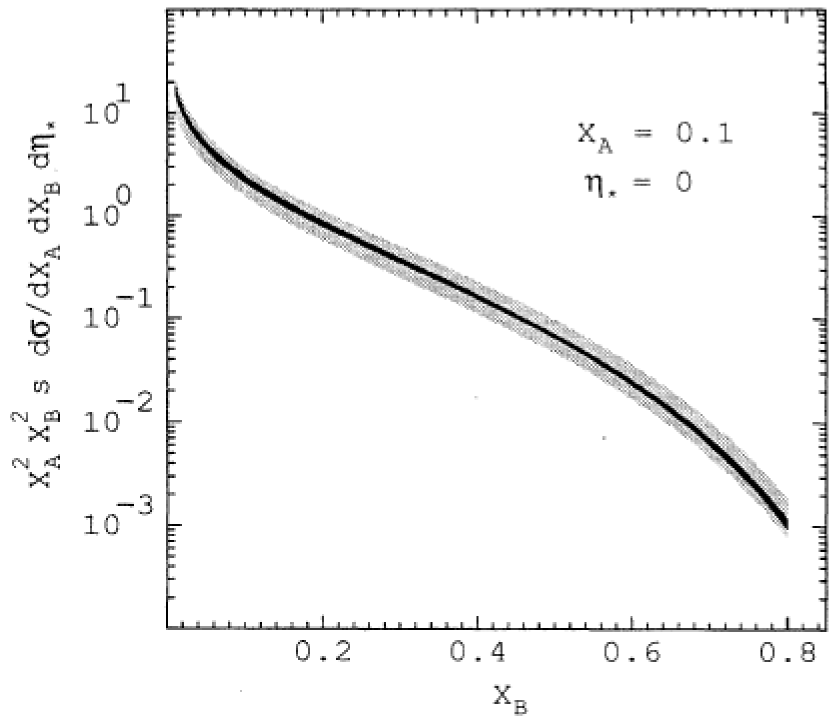

Ellis, Soper, PRL 74, 5182 (1995).

$$V^{(3)} = \{X_B, X_A, y^*\}$$

$$X_A = \sum_{n \in \text{dijets}} \frac{E_{Tn}}{\sqrt{s}} e^{+y_n}$$

$$X_B = \sum_{n \in \text{dijets}} \frac{E_{Tn}}{\sqrt{s}} e^{-y_n}$$

LO: $X_A = \mathrm{x_p}$ control the probe

$X_B = \mathrm{x_{Pb}}$ scan the target

A kinematic scanning of initial state with dijet configuration

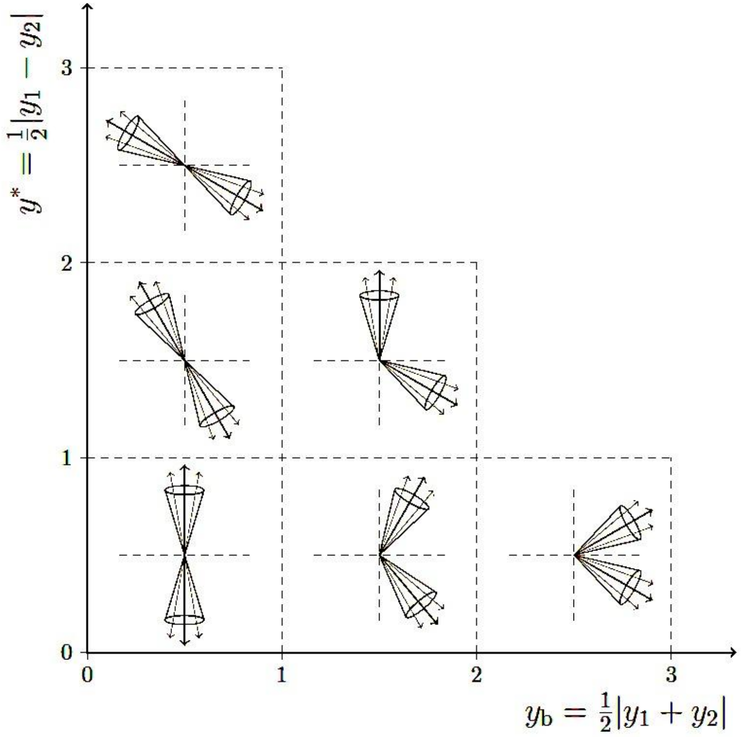

Part 2: Construction of the image of $r_i^A(x, Q^2)$ in pA

Dijet in pA

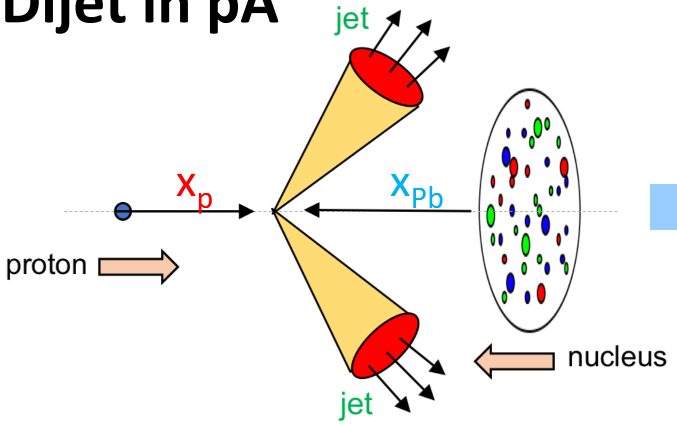

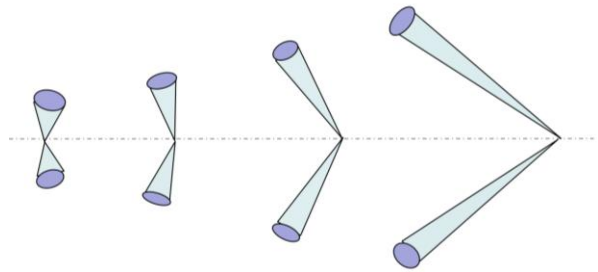

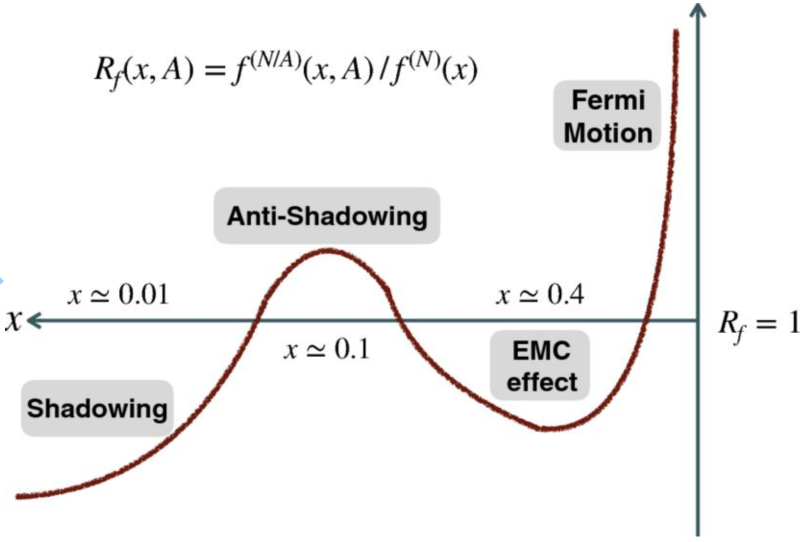

Shen, Ru, Zhang, PRD 105, 096025 (2022)

More advantages in pPb collisions

$$R_{pA}(v_1,v_2,v_3) \approx \frac{\sum_{a,b} f_a^p(x_a,\mu^2) f_b^A(x_b,\mu^2) H_{ab}(v_1,v_2,v_3)}{\sum_{a,b} f_a^p(x_a,\mu^2) f_b^p(x_b,\mu^2) H_{ab}(v_1,v_2,v_3)}$$

$r_i^A(x, Q^2)$

1. Uncertainties from proton PDFs reduced.
2. Uncertainties from high-order corrections reduced.
3. Incoming from one side.
4. Experimental uncertainties also reduced.

Part 2: Construction of the image of $r_i^A(x, Q^2)$ in pA

Extended to cases with fixed probing scales.

$$V^{(3)} = \{X_B, E_T^{JJ}, p_T^{avg}\} \quad E_T^{JJ} = \sqrt{M_{JJ}^2 + (\vec{p}_{T1} + \vec{p}_{T2})^2}$$

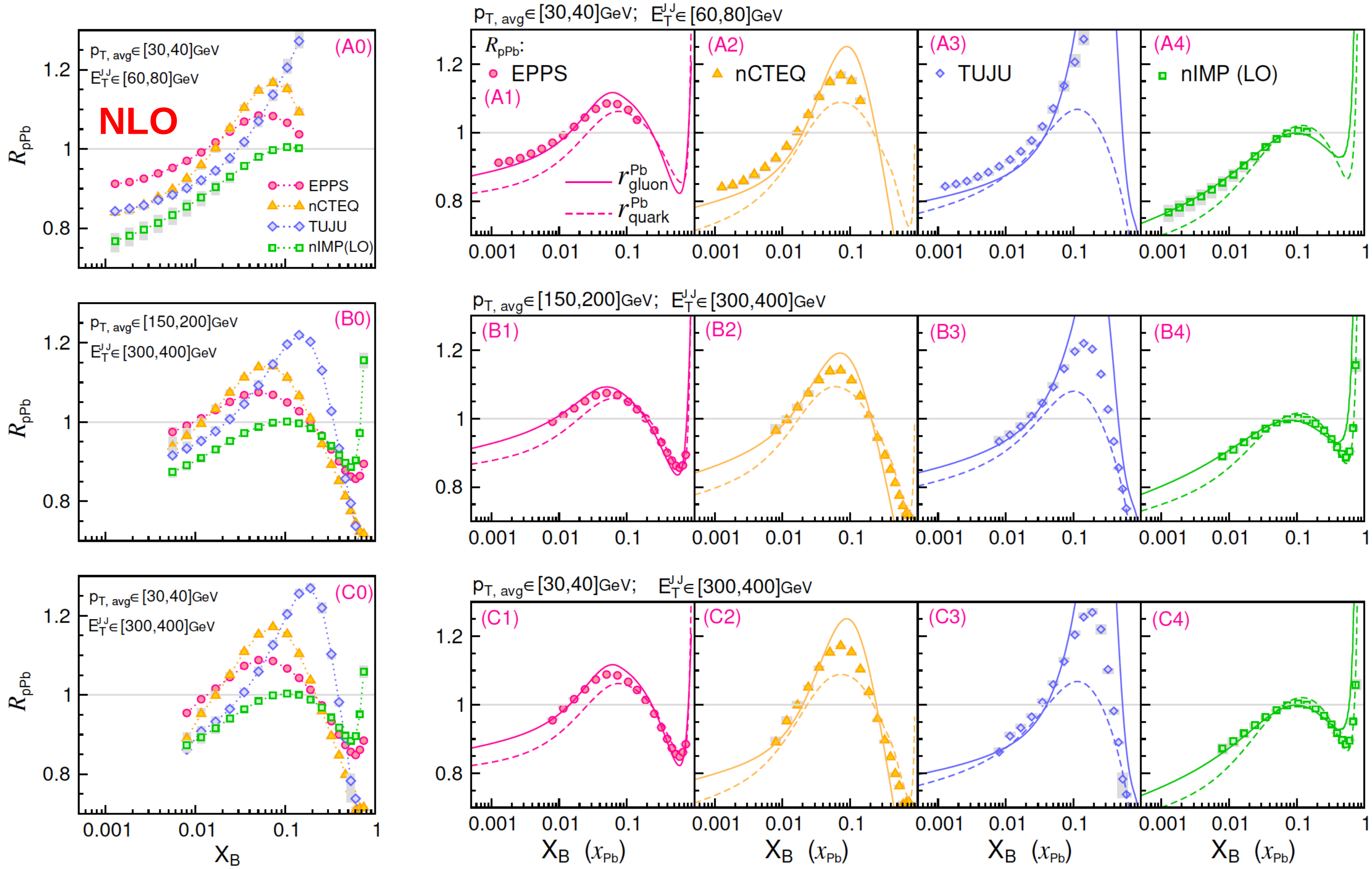

Shen, Ru, Zhang, PRD 105, 096025 (2022)

Part 2: Construction of the image of $r_i^A(x, Q^2)$ in pA

Extended to cases with fixed probing scales.

$$V^{(3)} = \{X_B, E_T^{JJ}, p_T^{avg}\} \quad E_T^{JJ} = \sqrt{M_{JJ}^2 + (\vec{p}_{T1} + \vec{p}_{T2})^2}$$

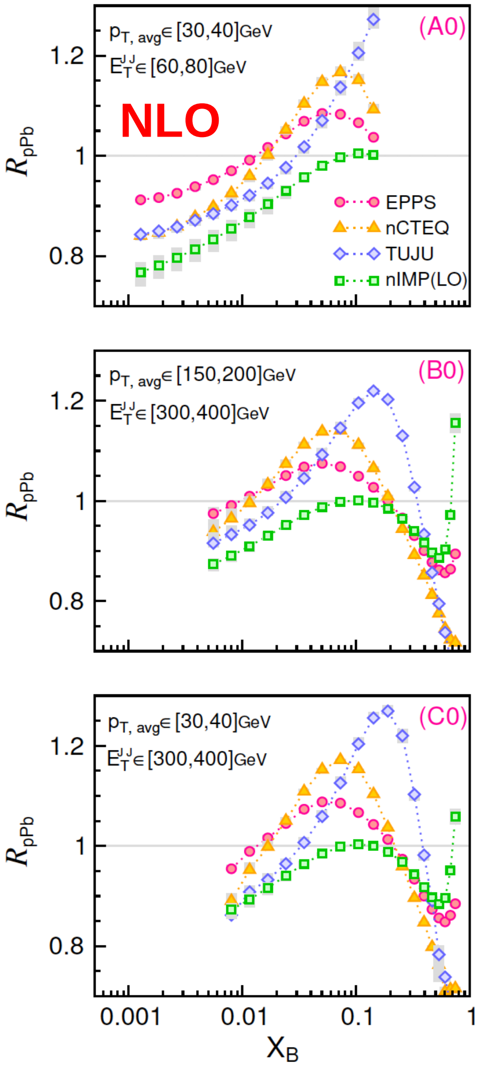

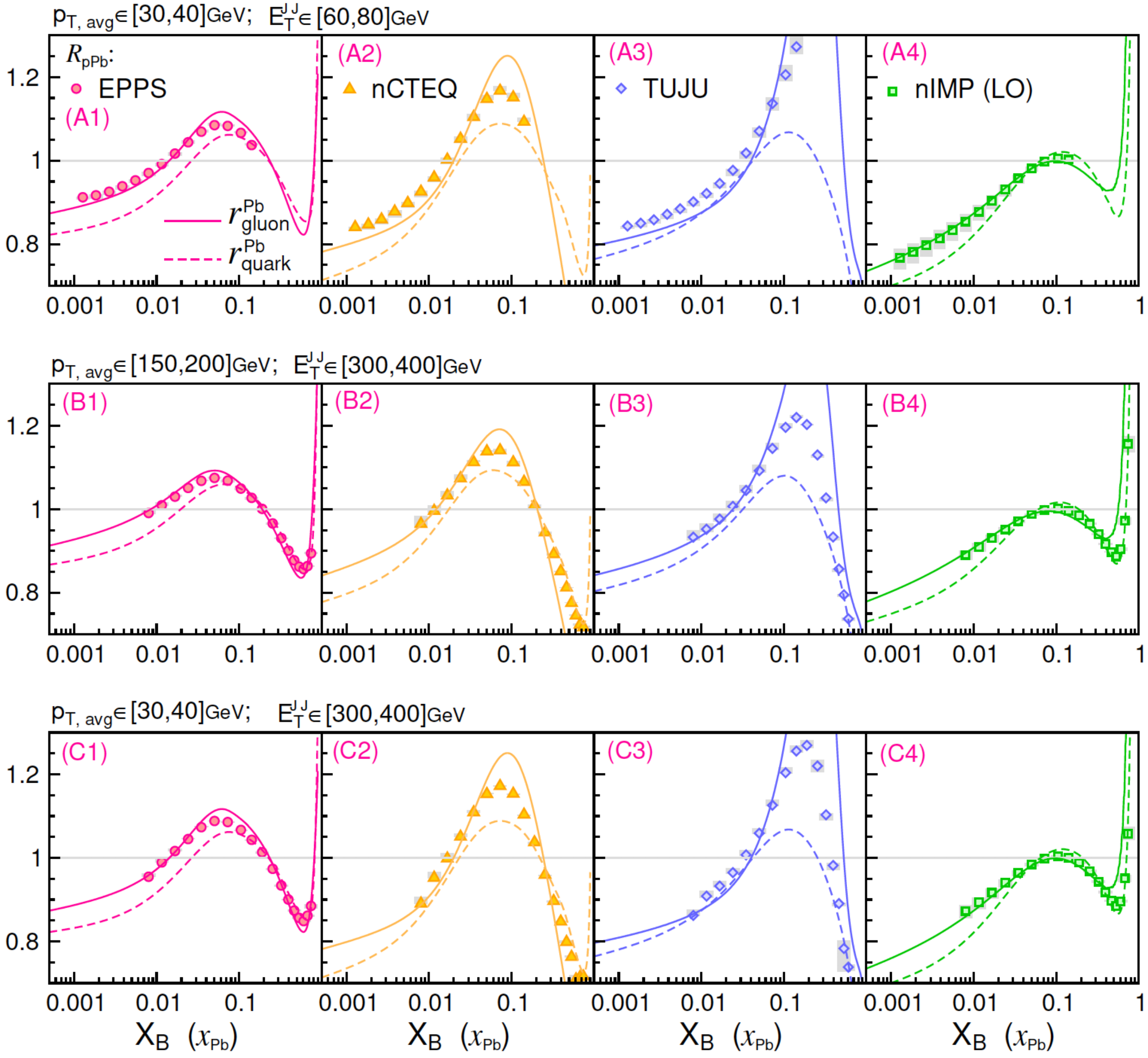

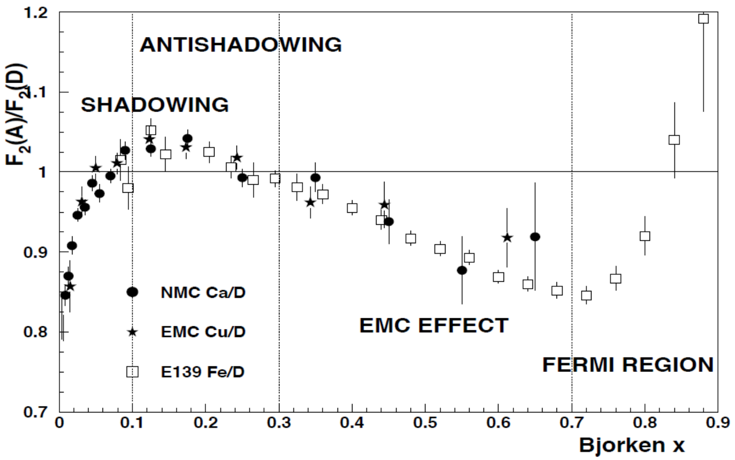

1. Scanning of $r_i^A(x, Q^2)$ in pA, verified at NLO.

2. An analogy to the image in DIS.

3. However, parton flavors are still mixed.

Shen, Ru, Zhang, PRD 105, 096025 (2022)

Part 2: Construction of the image of $r_i^A(x, Q^2)$ in pA

Can parton flavors can be further separated?

Multi-process imaging based on the scanning with (x, Q^2)

Part 2: Construction of the image of $r_i^A(x, Q^2)$ in pA

Can parton flavors can be further separated?

Multi-process imaging based on the scanning with (x, Q^2)

Process	Partonic subprocess at LO
Z-boson	$q + \bar{q} \to Z \to l^+ l^-$
$Z +$ jet	$q + \bar{q} \to Z + g$ $q(\bar{q}) + g \to Z + q(\bar{q})$
$Z + c$-jet	$c(\bar{c}) + g \to Z + c(\bar{c})$

Part 2: Construction of the image of $r_i^A(x, Q^2)$ in pA

Can parton flavors can be further separated?

Multi-process imaging based on the scanning with (x, Q^2)

Process	Partonic subprocess at LO
Z-boson	$q + \bar{q} \to Z \to l^+ l^-$
$Z +$ jet	$q + \bar{q} \to Z + g$ $q(\bar{q}) + g \to Z + q(\bar{q})$
$Z + c$-jet	$c(\bar{c}) + g \to Z + c(\bar{c})$

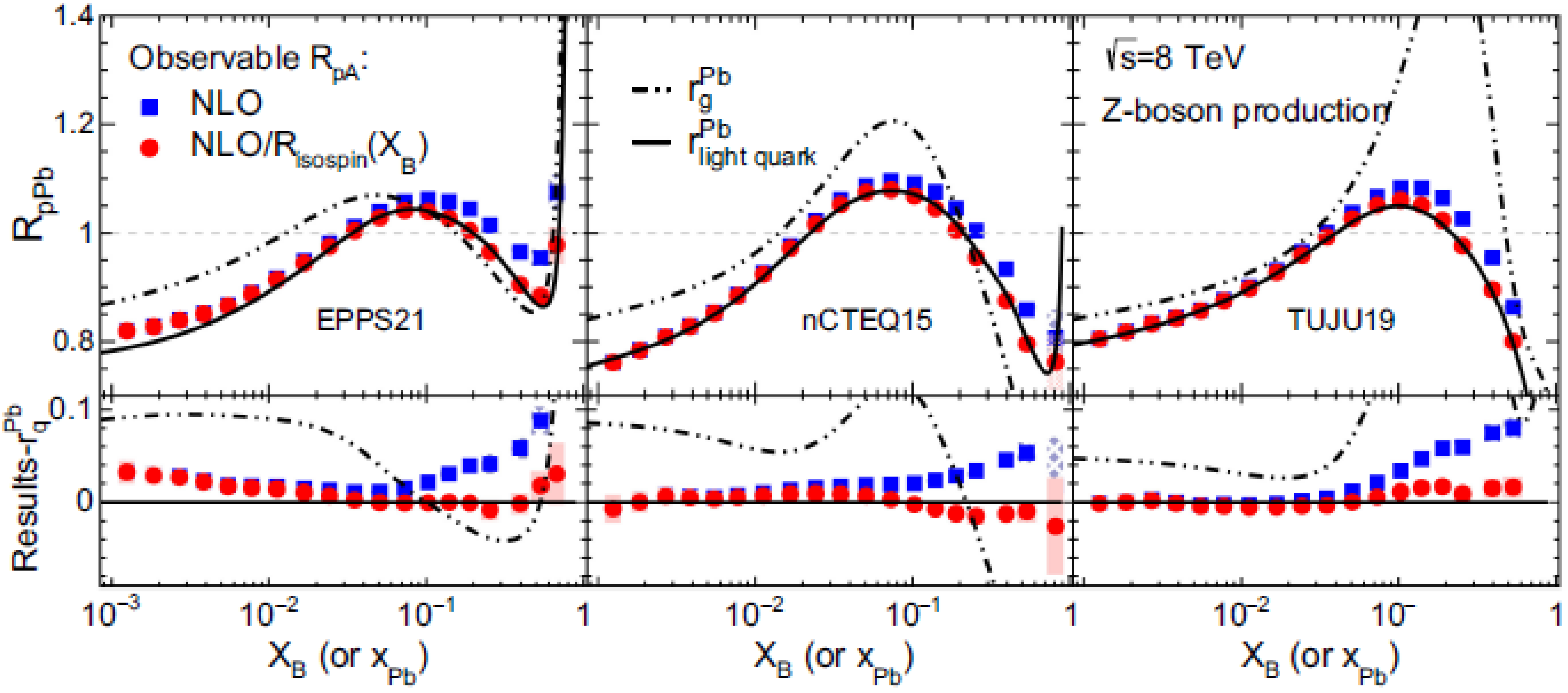

Z-boson nicely images the $r_i^A(x, Q^2)$ for light quarks!

Yang, Ru, Zhang, PRD 112, 074008 (2025)

Part 2: Construction of the image of $r_i^A(x, Q^2)$ in pA

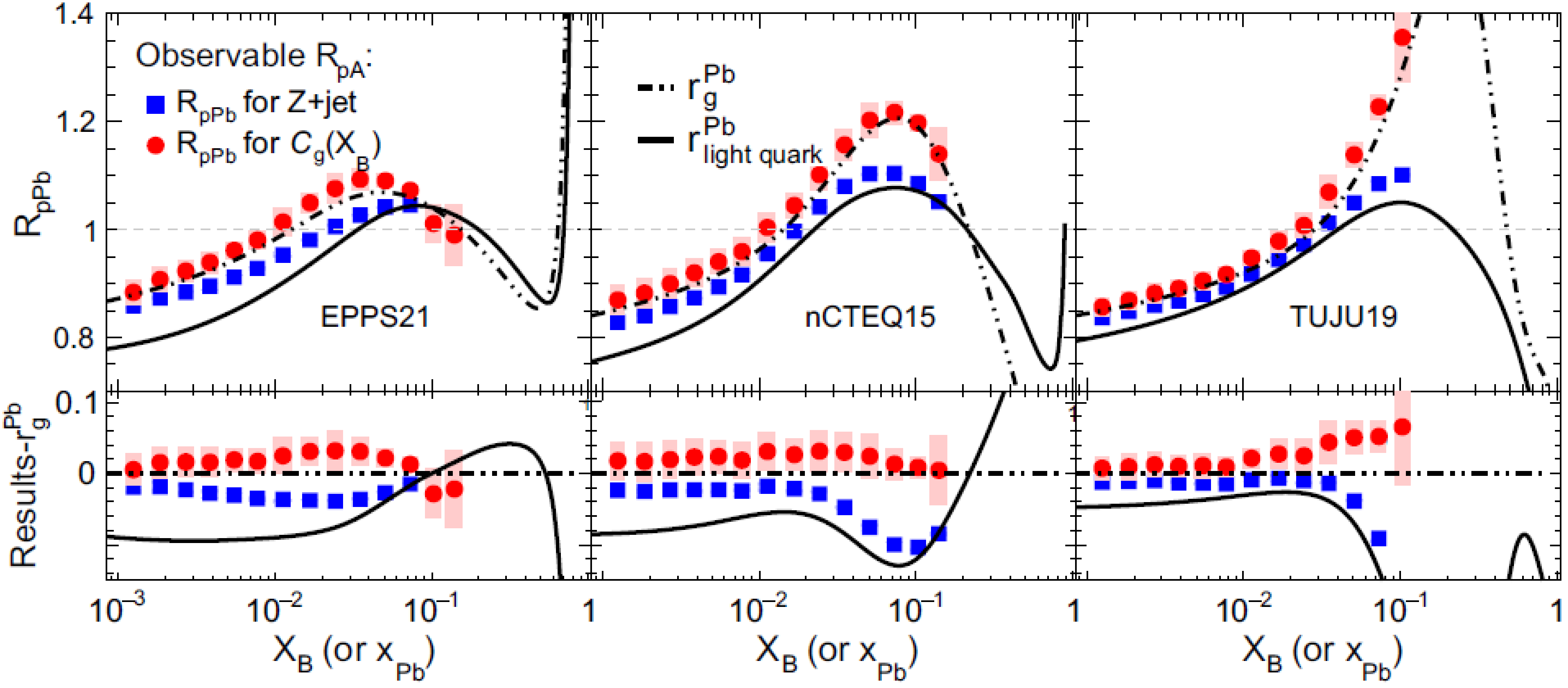

Z+jet images the mixture of $r_i^A(x, Q^2)$ for light quarks and gluons.

Yang, Ru, Zhang, PRD 112, 074008 (2025)

Part 2: Construction of the image of $r_i^A(x, Q^2)$ in pA

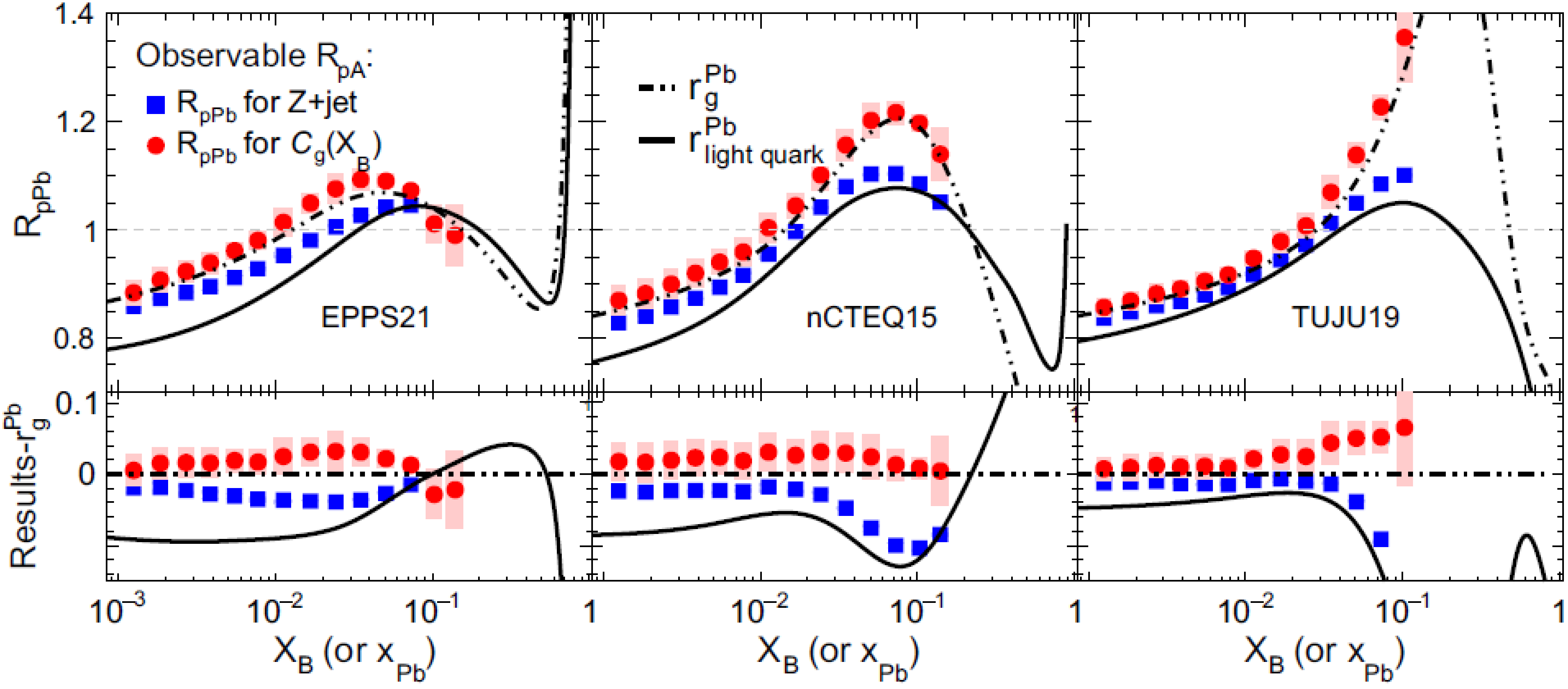

Z+jet images the mixture of $r_i^A(x, Q^2)$ for light quarks and gluons.

Yang, Ru, Zhang, PRD 112, 074008 (2025)

A combined observable with Z-boson and Z+jet:

$$C_g(X_B) = \kappa_1(X_B) \times d\sigma^{Z+\mathrm{jet}}(X_B) - d\sigma^Z(X_B) \qquad \kappa_1(X_B) = \frac{d\sigma^Z(X_B)}{[d\sigma^{Z+\mathrm{jet}}(X_B)]_{\mathrm{nuclear\ quark}}}.$$

which suppresses the effects from nuclear quarks and nicely images the $r_i^A(x, Q^2)$ for gluons!

Part 2: Construction of the image of $r_i^A(x, Q^2)$ in pA

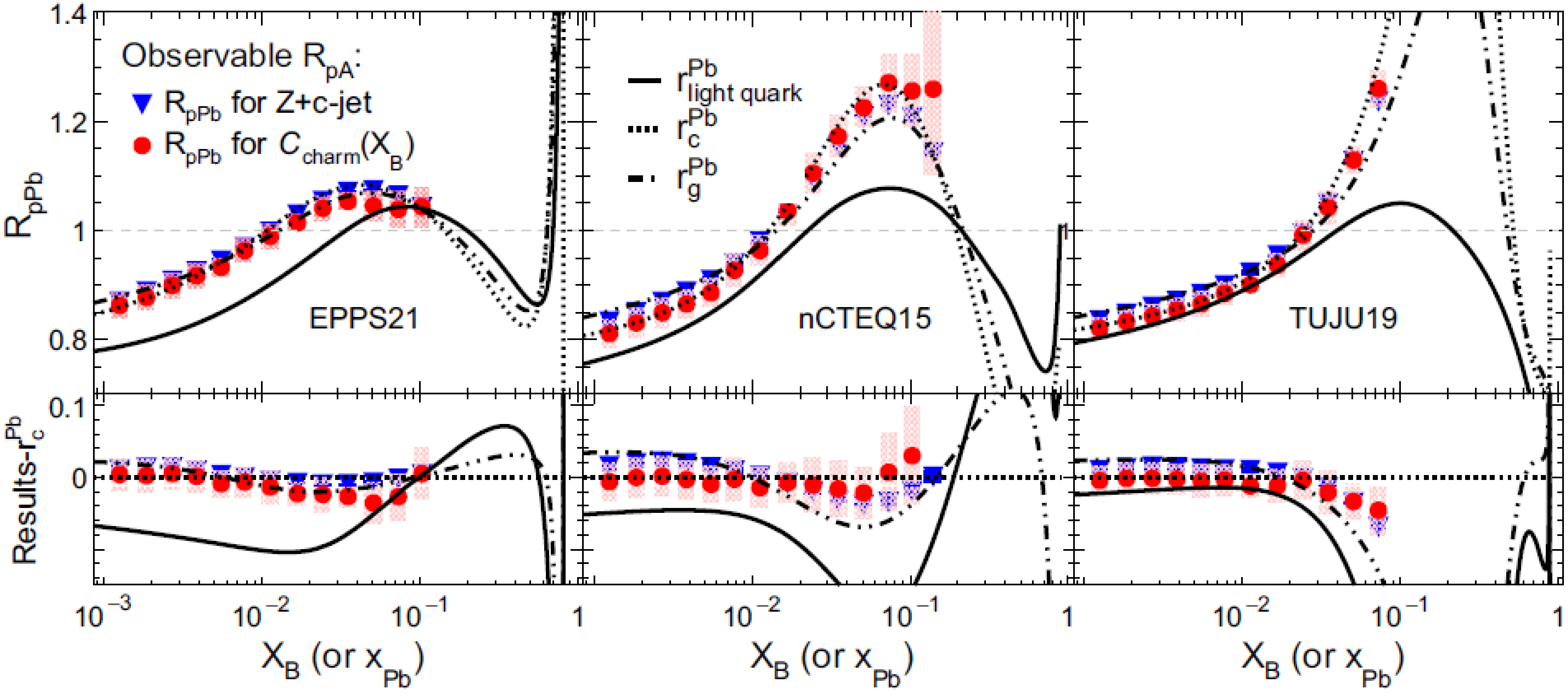

Z+c-jet images the mixture of $r_i^A(x, Q^2)$ for charm quarks and gluons.

Yang, Ru, Zhang, PRD 112, 074008 (2025)

A combined observable with Z-boson & Z+jet & Z+c-jet:

$$C_{charm}(X_B) = \kappa_2(X_B) \times d\sigma^{Z+c\text{-jet}}(X_B) - C_g(X_B)$$

which nicely images the $r_i^A(x, Q^2)$ for charm quarks!

Part 2: Construction of the image of $r_i^A(x, Q^2)$ in pA

Yang, Ru, Zhang, PRD 112, 074008 (2025)

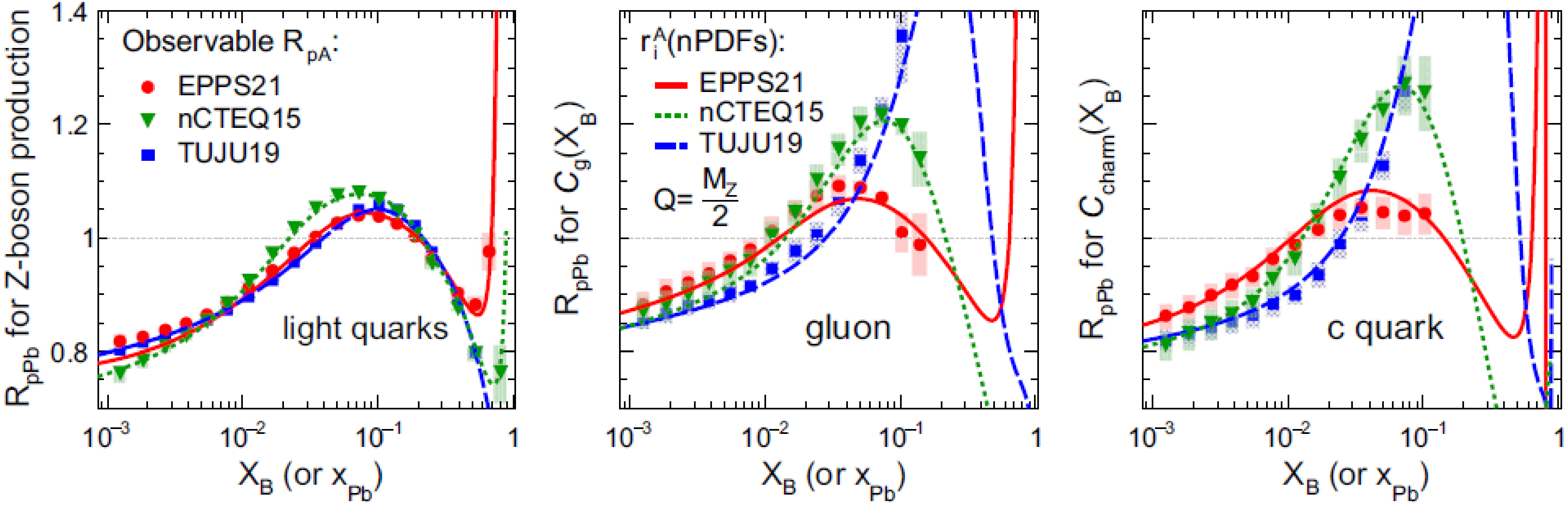

The results show the probability to separately image of $r_i^A(x, Q^2)$ for certain parton flavors at the LHC.

Other processes at the LHC

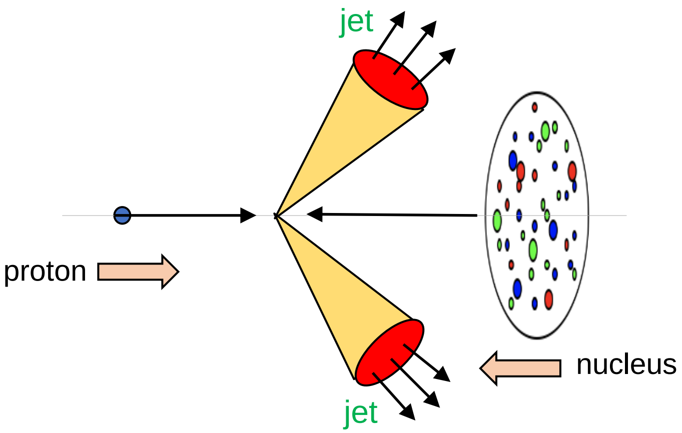

Dijet, Drell-Yan, γ-jet, ……

Combined study of LHC and EicC/EIC

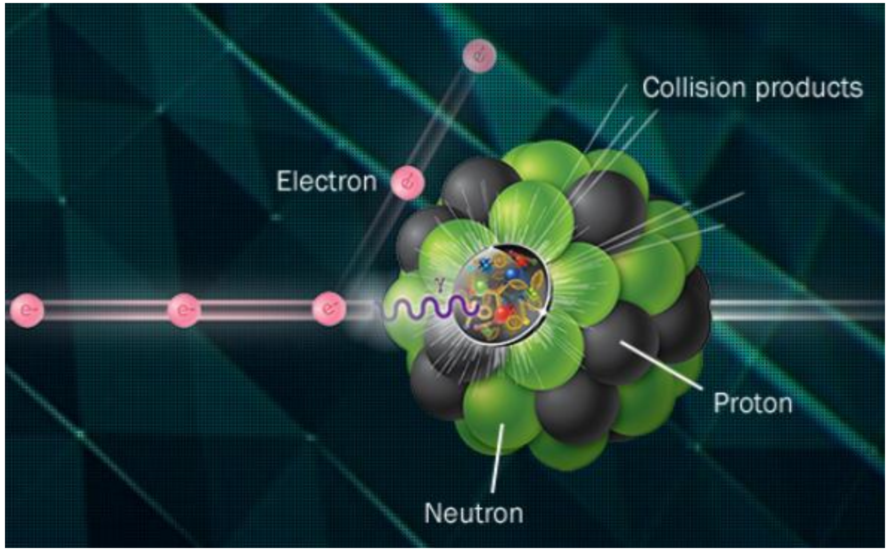

Systematic comparison spanning from pA to eA

Part 3: Future applications

Extended to spin & 3D structure

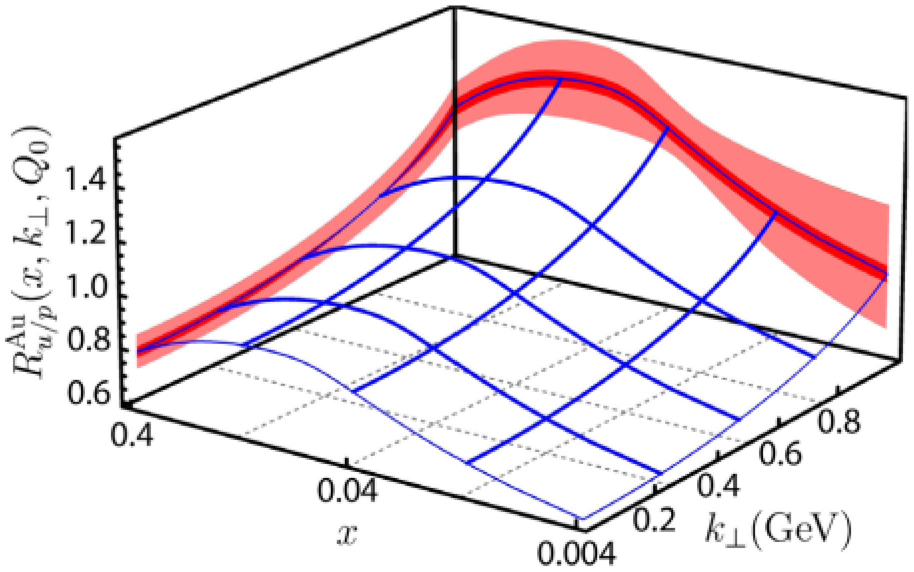

Alrashed, Anderle, Kang, Terry, Xing
PRL 129, 242001 (2022)

Nuclear effects at higher-twist

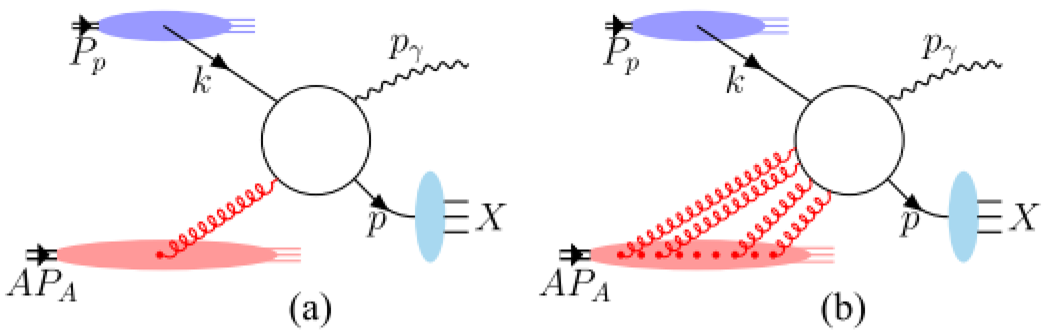

Fu, Kang, Salazar, Wang, Xing
PRL 135, 032301 (2025)

Part 4: Summary & Discussion

An imaging methodology is developed to optimize the future measurements at the LHC.

-With better disentangled contributions of (x, Q^2, i) for nuclear modification $r_i^A(x, Q^2)$

-Facilitate more efficient global analysis

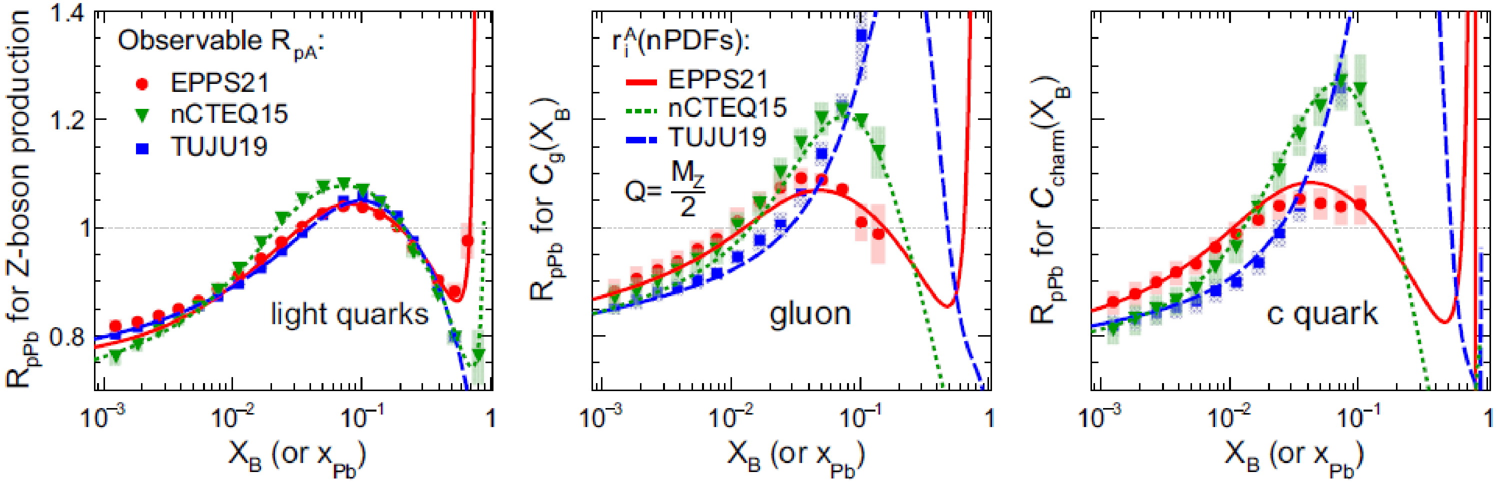

Part 4: Summary & Discussion

An imaging methodology is developed to optimize the future measurements at the LHC.

-With better disentangled contributions of (x, Q^2, i) for nuclear modification $r_i^A(x, Q^2)$

-Facilitate more efficient global analysis

Neither PDFs nor $r_i^A(x, Q^2)$ is directly measurable!

- Compared to traditional observables, the proposed imaging observables provide somewhat preprocessed data with theoretical guidance.

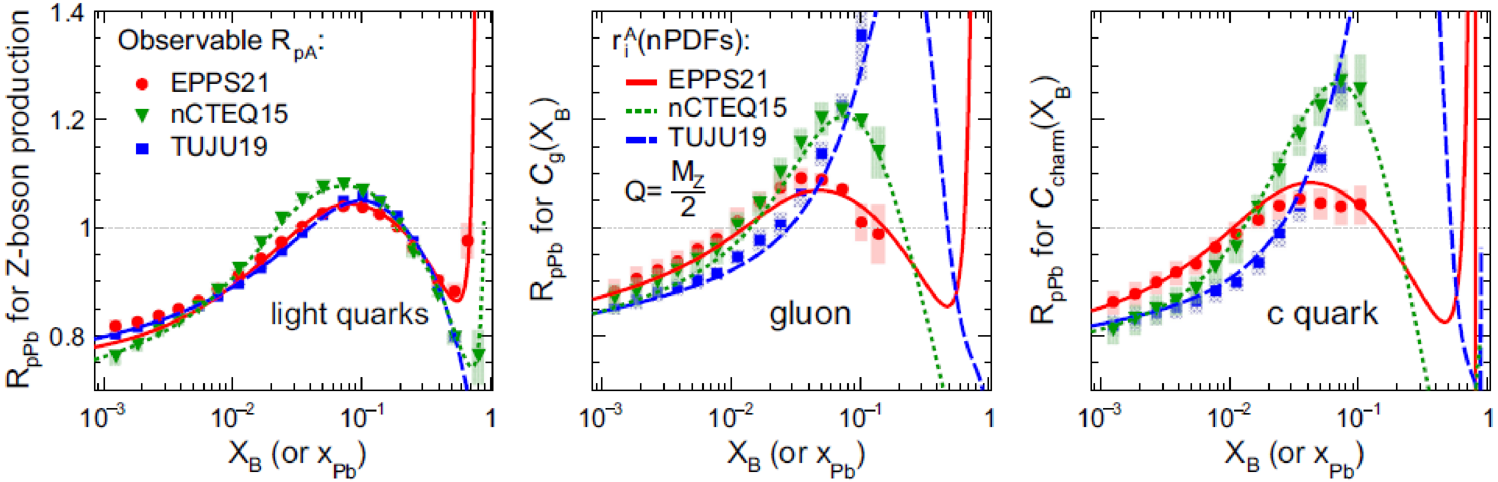

Part 4: Summary & Discussion

An imaging methodology is developed to optimize the future measurements at the LHC.

-With better disentangled contributions of (x, Q^2, i) for nuclear modification $r_i^A(x, Q^2)$

-Facilitate more efficient global analysis

Neither PDFs nor $r_i^A(x, Q^2)$ is directly measurable!

- Compared to traditional observables, the proposed imaging observables provide somewhat preprocessed data with theoretical guidance.

Thanks for your attentions!

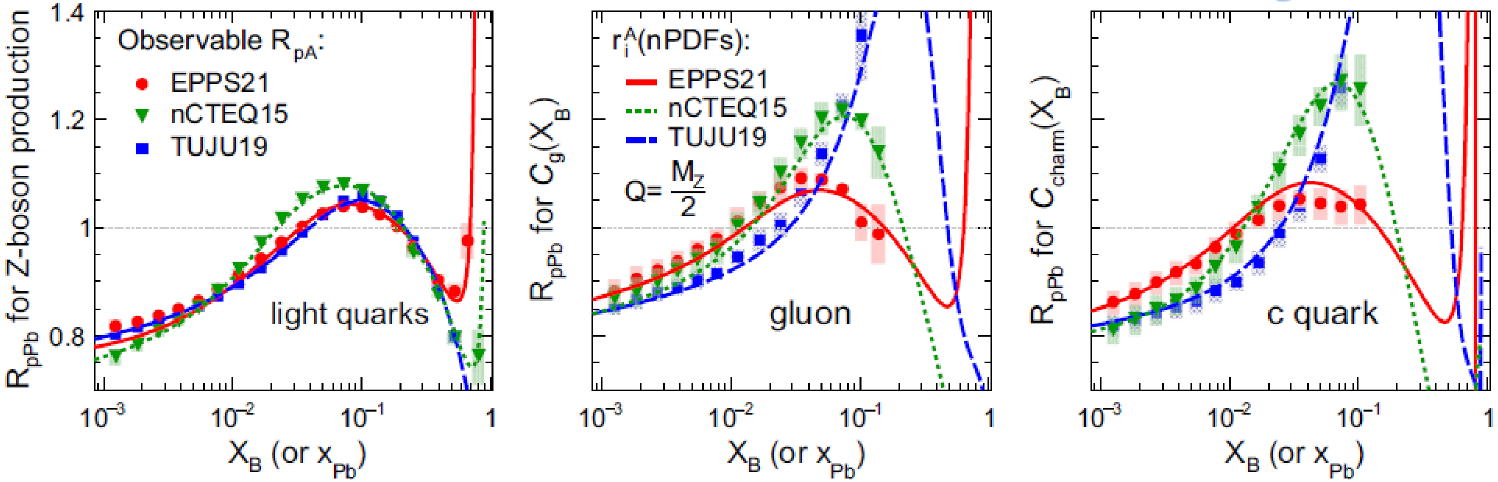

Backup

Examine the results with fixed factorization scale at NLO & LO